

1 **Short Title:** MiR5628 enhances decay of *PYL6* mRNA in response to ABA

2

3 **Corresponding author:** Michel Vincentz, Center for Molecular Biology and Genetic
4 Engineering, University of Campinas, Zip code 13083-875, mailbox 6010, Campinas, São
5 Paulo, Brazil. Tel +55 19-3521-1089. Email for contact mgavince@unicamp.br.

6

7 **Regulation of *PYR/PYL/RCAR* ABA receptors mRNA stability: involvement of
8 miR5628 in decay of *PYL6* mRNA**

9

10 João G. P. Vieira¹, Gustavo T. Duarte^{1,2}, Carlos H. Barrera-Rojas³, Cleverson C. Matioli¹,
11 Américo J. C. Viana¹, Lucas E. D. Canesin⁴, Renato Vicentini⁵, Fabio T. S. Nogueira³ and
12 Michel Vincentz ¹.

13

14 ¹ Laboratory of Plant Genetics, Center for Molecular Biology and Genetic Engineering,
15 University of Campinas, 13083-875, Campinas, São Paulo, Brazil.

16 ² Belgian Nuclear Research Centre (SCK CEN), Unit for Biosphere Impact Studies,
17 Boeretang 200, 2400, Mol, Belgium.

18 ³ Laboratory of Molecular Genetics of Plant Development, Department of Biological
19 Sciences, *Escola Superior de Agricultura 'Luiz de Queiroz'*, University of São Paulo,
20 Piracicaba, São Paulo, 13418-900, Brazil.

21 ⁴ Genomics for Climate Change Research Group, Center for Molecular Biology and
22 Genetic Engineering, University of Campinas, 13083-875, Campinas, São Paulo, Brazil.

23 ⁵ Systems Biology Laboratory, Department of Plant Genetics and Breeding, University of
24 Campinas, 13083-862, Campinas, São Paulo, Brazil.

25

26 **One Sentence Summary:** Attenuation of ABA signaling involves destabilization of
27 *PYL1/4/5/6* transcripts. ABA core signaling induces miR5628 expression to enhance
28 *PYL6* mRNA degradation in conjunction with decapping and XRN4 activities.

29

30 **Authors Contribution:**

31 J.G.P.V. designed, performed and analyzed the data of all experiments but dual-luciferase
32 assay, wrote and edited the manuscript.

33 G.T.D. designed experiments, carry out cordycepin and long-term ABA kinetics
34 experiments and edited the manuscript.

35 C.C.M and A.J.C.V. designed experiments and edited the manuscript.

36 C.H.B.R and F.T.S.N. edited the manuscript, designed and carry out dual-luciferase assay
37 experiments and generate the transgenic plants overexpressing the microRNA5628.

38 L.E.C.C and R.V. carry out the bioinformatics analyses.

39 M.V. obtained funding, supervised the project, designed and analyzed the data of all
40 experiments, wrote and edited the manuscript.

41

42 **Funding:** This work was funded by Sao Paulo Research Foundation (FAPESP): M.G.A.V.
43 (grant 2015/25838-2), J.G.P.V. (grant 2016/0498-7 and 2019/25696-4), G.T.D. (grant
44 2012/22125-7).

45

46 **ABSTRACT**

47 Hormone signaling fine-tuning involves feedback regulatory loops. Abscisic acid (ABA)
48 plays key functions in development and tolerance to abiotic stress. ABA is sensed by the
49 PYR/PYL/RCAR receptors and it also represses their gene expression. Conversely, ABA
50 induces *PP2C* phosphatases expression, which are negative regulators of the ABA
51 signaling pathway. This feedback regulatory scheme is likely important for the
52 modulation of ABA signal transduction. Here, we provide a new insight into the
53 mechanisms underlying the ABA-induced negative control of *PYR/PYL/RCAR* expression
54 in *Arabidopsis thaliana*. The strong and sustained repression of *PYR/PYL/RCARs*
55 revealed by ABA time course treatment defines the regulation of receptors genes as an
56 important step in resetting the ABA signaling pathway. Transcription inhibition by
57 cordycepin showed that destabilization of *PYL1/4/5/6* mRNA is involved in ABA-
58 induced repression of these genes. Furthermore, genetic evidence indicated that
59 decapping may play a role in *PYL4/5/6* mRNAs decay. In addition, we provide evidence
60 that the *Arabidopsis*-specific microRNA5628 (miR5628), which is transiently induced by
61 the ABA core signaling pathway, guides the cleavage of *PYL6* transcript in response to
62 ABA. After cleavage, the resulting RISC 5'- and 3'-cleaved fragments of *PYL6* mRNA may
63 be degraded by exoribonuclease XRN4. MiR5628 is an evolutionary novelty that may
64 contribute, with decapping and XRN4 activities, to enhance *PYL6* mRNA degradation.
65 Thus, control of stability of *PYR/PYL/RCAR* transcripts is an important step in
66 maintaining homeostasis of ABA signaling.

67

68 **KEY WORDS:** Abscisic acid, negative feedback, homeostasis, mRNA decay, ABA
69 signaling, microRNA, XRN4, decapping and exoribonuclease activity.

70

71 **INTRODUCTION**

72 To adjust their physiology and growth in response to constant environmental
73 changes, plants developed mechanisms to sense and transduce external and endogenous
74 signals into adequate growth and developmental responses. This ability of a biological
75 system to regulate its internal state in the face of external perturbations is known as
76 homeostasis (Somvanshi et al., 2015). Control of homeostasis is the standard in
77 hormone responses, whereby the signaling cascade must be dampened after an initial
78 trigger to avoid overreactions. Such a control involves feedback loops. For instance,

79 auxin, gibberellin, ethylene, strigolactone, cytokinin and brassinosteroids signaling are
80 known to trigger the activation of negative regulators as part of the responses induced
81 by these hormones (Teale et al., 2006; Davière and Achard, 2013; Zhu et al., 2013; Rai et
82 al., 2015; Waters et al., 2017; Kieber and Schaller, 2018).

83 Similarly, the modulation of abscisic acid (ABA) signaling also involves the
84 induction of negative regulators (*i.e.*, *PP2C* phosphatases) and downregulation of
85 positive regulators (*i.e.*, *PYR/PYL/RCAR* ABA receptors), as part of the feedback loop for
86 the attenuation of the hormone signal transduction (Song et al., 2016). Basal ABA levels,
87 which range from 6 to 32 nM in *Arabidopsis thaliana*, support plant growth and
88 development via a beneficial effect on water status of plants (Yoshida et al., 2019), while
89 higher level of ABA plays an important role in responses to abiotic stress conditions
90 such as drought, heat, cold and high salinity (Kavi Kishor et al., 2022). In *A. thaliana*, the
91 ABA core signaling pathway is composed by 14 ABA receptors *PYRABACTIN*
92 *RESISTANCE 1 (PYR1)/PYR1-LIKE (PYL)/REGULATORY COMPONENT OF ABA*
93 *RECEPTOR (PYR/PYL/RCAR)*, classified into three subgroups; nine clade A type 2C,
94 *PROTEIN PHOSPHATASES (PP2C)*; and three *SNF1*-related protein kinases 2 from
95 subclass III (*SnRK2*) (Ma et al., 2009; Park et al., 2009). In the absence of ABA, *PP2Cs*
96 continuously inhibit the signaling pathway by repressing *SnRK2s* activity (Ma et al.,
97 2009; Park et al., 2009). The *PYR/PYL/RCAR* receptors of subgroup I have higher
98 affinity for ABA than subgroups II and III, which respond to higher ABA levels (Tischer
99 et al., 2017; Yoshida et al., 2019). Thus, subgroup I *PYR/PYL/RCAR* would be more
100 involved in growth processes, while subgroups II and III would have a more prominent
101 role under stress conditions, when ABA levels can increase up to 30-fold (Urano et al.,
102 2017). In either case, ABA is perceived by *PYR/PYL/RCARs*, which inhibit the *PP2Cs*,
103 thus releasing *SnRK2* kinases from the negative regulation (Ma et al., 2009; Park et al.,
104 2009). These kinases then can trigger changes in gene expression by activating ABA-
105 responsive transcription factors and by modulating the activity of protein complexes
106 involved in mRNA stability control (Wang et al., 2013).

107 The control of mRNA stability is an important mode of regulation of
108 *PYR/PYL/RCAR* and *PP2C* expression (Wang et al., 2015; Wawer et al., 2018). In *A.*
109 *thaliana*, cytoplasmic mRNA turnover pathway is initiated by poly(A) tail shortening.
110 Next, the deadenylated mRNA may either be channeled into the 3'-5' mRNA decay
111 pathway, which involves degradation by the exosome, or be targeted by the 5'-3' mRNA

112 decay pathway, which consists of the DECAPPING 2 (DCP2) enzyme and its activators
113 DCP1, DCP5, VARICOSE, and PAT1. Finally, 5'-decapped transcripts are degraded by the
114 exoribonuclease XRN4 (Chantarachot and Bailey-Serres, 2018). This mRNA turnover
115 pathway is conserved among eukaryotes (Mugridge et al., 2018). Alternatively,
116 transcripts degradation can be triggered by microRNAs (miRNAs) pathways. MiRNAs
117 biogenesis begins with the transcription of MIR genes, by RNA polymerase II, generating
118 a primary transcript (pri-miRNA). This transcript generates a hairpin-shaped secondary
119 structure that is processed by DICER-LIKE1 (DCL1) generating a miRNA-miRNA duplex.
120 This duplex is methylated by HEN1 to be transported from the nucleus to the cytoplasm.
121 One of the strands of the duplex is incorporated into the Interfering RNA Silencing
122 Complex (RISC). In the cytoplasm, the miRNA will recognize its target by base
123 complementarity, cleaving it by Argonaut, or repressing translation (Barrera-Rojas et al.,
124 2021).

125 Our previous observation that ABA and glucose act in synergy to destabilize the
126 mRNA of the transcription factor *bZIP63* (Matiolli et al., 2011), prompted us to
127 investigate the impact of ABA on the control of mRNA stability at genomic scale.
128 Interestingly, we noticed that ABA promotes the destabilization of *PYL4*, *PYL5* and *PYL6*
129 receptors transcripts. Here, we confirm that ABA accelerates the decay of these
130 transcripts. We provide evidence that the ABA core signaling pathway induces the
131 *Arabidopsis*-specific miR5628 expression in response to ABA, which in turn promotes
132 *PYL6* mRNA cleavage and mRNA decay in a XRN4-dependent way. Moreover, decapping
133 was also found to be involved in the control of *PYL4/5/6* receptors mRNA decay in
134 response to ABA. The control of the stability of *PYR/PYL/RCAR* transcripts is proposed
135 to be part of a feedback regulatory loop participating in the attenuation and resetting of
136 the ABA signaling.

137

138 RESULTS

139 **Negative feedback of ABA signaling involves sustained repression of** 140 ***PYR/PYL/RCAR* gene expression**

141 Regulatory feedback acting upon the ABA signaling pathway has been described
142 (Song et al., 2016). To obtain new insight into the underpinning mechanism, we set-up
143 an experimental design to evaluate the response of the ABA core signaling pathway
144 genes in response to 1 μ M ABA, which is likely to mimic abiotic stress conditions

145 (Tischer et al., 2017; Urano et al., 2017). We have analyzed the expression profile of
146 seven of the fourteen representative members of *PYR/PYL/RCAR* receptors multigene
147 family (Supplemental Fig. S1A). We also have measured the expression of six
148 representative members of *PP2C* phosphatases and all three *SnRK2* kinases from
149 subclass III (Supplemental Fig. S1A). After one-hour of ABA treatment, the expression of
150 all seven *PYR/PYL/RCARs* were found to be repressed in response to the hormone
151 (Supplemental Fig. S1B). In contrast, the six *PP2Cs* phosphatases and *SnRK2.6* were
152 induced by ABA, while the other two members of the subclass III *SnRK2* kinases did not
153 respond (Supplemental Fig. S1B). Thus, our experimental conditions recapitulate the
154 ABA-induced regulation of ABA core signaling genes described earlier (Song et al.,
155 2016).

156 To further explore the dynamic regulation of this representative subset of the
157 ABA core signaling genes (Supplemental Fig. S1), we have analyzed the time course
158 changes of their mRNA profiles in response to prolonged (16 hours) and transient (30
159 minutes) ABA treatments. These treatments were meant to mimic ABA-mediated
160 responses to variable durations of stress exposure. ABA-treatment for 16 h resulted in a
161 continuous repression of all ABA receptors analyzed but *PYL1* (Fig. 1A; Supplemental
162 Fig. S2), while all *PP2Cs* and *SnRK2.6* genes were transiently induced between one and
163 four hours after the beginning of ABA treatment, followed by a gradual decrease and
164 stabilization of their mRNA levels (Fig. 1A; Supplemental Fig S2). *SnRK2.2* and *SnRK2.3*
165 were induced later in comparison to the other ABA core signaling elements (Fig. 1A).
166 The continuous repression of most *PYR/PYL/RCAR* in comparison to the transient
167 induction of the *PP2C* genes suggests that the negative regulatory feedback acting on the
168 control of *PYR/PYL/RCAR* expression has an important role in attenuating the ABA
169 signaling pathway. The induction of *SnRK2.2/3/6* by ABA possibly reflects a way to
170 amplify ABA-mediated stress responses.

171 The changes of ABA core signaling genes expression in response to short term
172 ABA application should give clues about how the pathway is reset to its steady state
173 levels (*i.e.*, how it recovers the original transcript amounts prior to ABA treatment).
174 Therefore, we have performed a transient ABA treatment for 30 min and monitored the
175 mRNA levels of the representative subset of ABA core signaling pathway genes for 16 h
176 following removal of the hormone (Fig. 1B; Supplemental Fig. S3). The maximum
177 response of all evaluated ABA core signaling transcripts occurred between the end of the

178 30 min of ABA treatment and 1 h after the hormone removal (Fig. 1B; Supplemental Fig.
179 S3). The only exceptions were *SnRK2.2* and *SnRK2.3*, which were not affected (Fig. 1B).
180 Within a time frame of eight hours after the transitory ABA treatment, *HAB1*, *PP2CA*,
181 *HAI2* PP2Cs and *SnRK2.6* transcripts recovered their original levels, and *ABI1*, *ABI2* and
182 *HAI1* transcripts clearly tend also to do so (Fig. 1B; Supplemental Fig. S3). On the other
183 hand, the representative receptors had a slightly different behavior, *PYR1*, *PYL1/4/5/6*
184 and *PYL8* showed a slow recovery rate of their original transcript levels, reaching at
185 most 60% their initial levels (Fig. 1B; Supplemental Fig. S3), while *PYL2* has not shown a
186 tendency to recover over this time period (Supplemental Fig. S3). These results suggest
187 that the control of ABA receptors gene expression is an important aspect of the reset
188 process of the ABA signaling pathway.

189 To address whether a functional ABA core signaling pathway is required to
190 trigger the feedback downregulation of the gene expression of ABA receptors, we have
191 adopted two approaches. First, we compared the expression of *PYR/PYL/RCAR* genes in
192 response to ABA between the wild-type (WT) and the dominant *abi1-1* mutant, which
193 maintains SnRK2s dephosphorylated and, therefore, is insensitive to ABA (Umezawa et
194 al., 2009). *Rd29B* is a readout gene for ABA signaling (Yoshida et al., 2015) and was
195 found to be two times less effectively induced by ABA in *abi1-1* than in the WT (Fig. 1C).
196 ABA-promoted repression of *PYL6* (Fig. 1C) and *PYR1*, *PYL2*, *PYL4*, *PYL5*, *PYL6* and *PYL8*
197 receptor genes is attenuated in the *abi1-1* mutant in comparison to the WT
198 (Supplemental Fig. S4).

199 The second approach consisted in evaluating the participation of subclass III
200 SnRK2 kinases in the negative feedback regulation of ABA receptors by global kinase
201 inhibition with staurosporine and by monitoring the SnRK2 double-mutant,
202 *snrk2.2/snrk2.3* (*snrk2d*), in which ABA responses are attenuated (Fujii et al., 2007).
203 Staurosporine was effective in reducing the induction of *Rd29B* by ABA, indicating that
204 inhibition of subclass III SnRK2 kinases was partially achieved (Supplemental Fig. S5). In
205 the presence of staurosporine, the repression of *PYL1*, *PYL2*, *PYL4*, *PYL5*, *PYL6* and *PYL8*
206 by ABA was significantly attenuated as compared to the control (Supplemental Fig. S5).
207 In addition, a weaker induction of the *ABI1*, *ABI2*, *HAI1* and *HAI2* phosphatase genes by
208 ABA in the presence of staurosporine was detected (Supplemental Fig. S5). The results
209 suggest that in response to ABA, subclass III SnRK2 kinases are required for efficient
210 repression and induction of *PYR/PYL/RCAR* and of clade A *PP2C* genes, respectively. As

211 expected, induction of *RD29B* by ABA was significantly reduced in *snrk2d* (Fig. 1D). The
212 ABA-promoted repression of *PYR1*, *PYL2*, *PYL4*, *PYL6* and *PYL8* receptors is attenuated
213 in *snrk2d* mutant in comparison to the WT (Fig. 1D; Supplemental Fig. S6), while *PYL1*
214 and *PYL5* showed a similar tendency (Supplemental Fig. S6). ABA-based *PYL6* repression
215 was more strongly attenuated in the *snrk2d* compared to the others receptor genes (Fig.
216 1D). These results further support the participation of SnRK2 in triggering repression of
217 most *PYR/PYL/RCAR* in response to ABA. Together, these data suggest the ABA-
218 promoted *PYR/PYL/RCAR* repression relies on a functional ABA signalosome.

219 Since *PYR/PYL/RCARs* emerge as key targets of the negative regulatory feedback
220 and resetting of the ABA signaling pathway, the mechanisms underlying the repression
221 of ABA receptors genes were further investigated. To distinguish transcriptional from
222 mRNA decay regulations, we blocked transcription with cordycepin and analyzed
223 changes of receptors mRNA levels. Since ABA-induced expression of *Rd29B* is known to
224 be mainly transcriptional, this gene was, therefore, used as a control to monitor the
225 efficiency of transcription inhibition by cordycepin (Matiolli et al., 2011). ABA-induced
226 up-regulation of *Rd29B* mRNA was found to be reduced by 93% by cordycepin,
227 indicating that transcriptional inhibition was efficient (Supplemental Table S3). *PYL8*
228 (subgroup I), *PYL4*, *PYL5*, *PYL6* (subgroup II), *PYR1*, *PYL1* and *PYL2* (subgroup III)
229 transcripts half-life were reduced by ABA to different extents (Supplemental Table S3).
230 ABA-induced decay of *PYL4*, *PYL5* and *PYL6* mRNAs (subgroup II) was more accentuated
231 than decay of receptors transcripts from subgroup I and III (Fig. 1E; Supplemental Table
232 S3 and Supplemental Fig. S7). *PYL6* mRNA is the most strongly destabilized transcript
233 with a half-life reduction around 50% (Fig. 1E, Supplemental Table S3). Together, these
234 observations indicate that the ABA-induced downregulation of *PYR/PYL/RCAR* members
235 expression relies, at least partly, on the control of the stability of their mRNAs.

236 Interestingly, *PYL6* was the only receptor for which ABA-promoted transcript
237 levels reduction was more pronounced in the absence of cordycepin (200-fold reduction
238 by ABA versus 77-fold reduction by ABA + cordycepin; Supplemental Table S3). This
239 result raised the possibility that ABA-induced *PYL6* mRNA decay requires
240 transcriptional induction by ABA of a regulatory factor that modulates *PYL6* transcript
241 stability. The hypersensitivity to ABA of different mutants affecting the miRNAs pathway
242 (Duarte et al., 2013) prompted us to examine the possibility that a miRNA, whose
243 expression would be induced by ABA, could be involved in *PYL6* mRNA destabilization.

244

245 **MiR5628 is involved in the control of *PYL6* mRNA stability in response to ABA**

246 To evaluate the involvement of the miRNA pathway in the control of *PYL6* mRNA
247 stability, we analyzed its expression in mutants defective in miRNA biogenesis (*hyl1-2*
248 and *se-1*) and activity (*ago1-25*). After ABA treatment, *PYL6* mRNA levels were 2.2, 1.7
249 and 2.2-fold higher in *hyl1-2*, *se-1* and *ago1-25*, respectively, when compared to the WT
250 (Supplemental Fig. S8). These results support the hypothesis that the miRNA pathway is
251 involved in the control of *PYL6* transcript stability.

252 Based on *in silico* prediction analyzes (psRNA-Target software), four putative
253 miRNAs which could recognize *PYL6* transcript were identified. MiR8175 could bind to
254 *PYL6* coding sequence, whereas miR5628, miR5021 and miR840-3p, could target the
255 3'UTR region of the transcript (Fig. 2A; Supplemental Fig. S9). 5'-RACE analyzes were
256 carried out to investigate whether these four miRNAs can guide the cleavage of *PYL6*
257 transcript. *SPL9*, which is a target of the conserved miR156 (Wang et al., 2009), was used
258 as positive control for ligation of the GeneRacer RNA oligo to the RISC 3'-cleaved
259 fragment (Supplemental Fig. S10A). After 30 minutes of ABA treatment, 5'-RACE
260 products were obtained for miR5628 (Supplemental Fig. S10A), but not for the other
261 three miRNAs. The 5'-RACE PCR product related to potential miR5628-guided cleavage
262 were cloned and sequenced. Three cloned 5'-RACE products were found to match
263 position 11 and one clone matched position 15 of miR5628 site in *PYL6* mRNA,
264 suggesting that, indeed, miR5628 guides *PYL6* mRNA cleavage (Fig. 2A). The 5'-end of
265 the remaining 43 sequenced clones matched sequences downstream to miR5628
266 recognition site (Fig. 2A) and may represent 5'-end products of XRN4 exoribonuclease
267 degradation. This hypothesis was supported by the observation that, after ABA
268 treatment, *PYL6* mRNA 3'UTR region accumulated more in *xrn4-5* mutant than in the WT
269 (Supplemental Fig. S10B). These results suggest that miR5628 promotes cleavage of
270 *PYL6* mRNA in the 3'UTR region and XRN4 degrades the RISC 3'-cleaved fragment of
271 *PYL6* mRNA.

272 Additionally, we analyzed the expression of a transgenic line (Col-0 background)
273 expressing a fusion between *Green Fluorescent Protein* (GFP) and the coding sequence of
274 *PYL6* under the control of the 35S promoter but lacking the *PYL6*-3'UTR sequence
275 (*oxPYL6*), which contains the miR5628 target site (Fig. 2B). Quantification of
276 endogenous *PYL6* mRNA using primers covering its 3'UTR showed that in both WT and

277 *oxPYL6*, the native *PYL6* transcripts are equally downregulated by ABA (Fig. 2B). Using
278 *PYL6* coding sequence (CDS)-specific primers, two-times more *PYL6*-CDS mRNA
279 sequences were detected in *oxPYL6* than in the WT because the *PYL6*-CDS-specific
280 primers amplify the endogenous *PYL6* and the *GFP:PYL6* fusion transcripts (Fig. 2B). Yet,
281 ABA treatment promoted only a three-fold reduction of *PYL6*-CDS mRNA in *oxPYL6* as
282 compared to a 54-fold repression in the WT (Figure 2B). Since promoter 35S is not
283 regulated by ABA (Chu and Jeng, 2002), this difference is not due to ABA-mediated
284 transcriptional effect and could, therefore, be a consequence of the inability of mRNA
285 decay regulations to act on the *GFP:PYL6* fusion transcript which lacks the 3'UTR region
286 (Fig. 2B). This possibility is supported by the observation that the GFP-mRNA sequence
287 is only marginally repressed by ABA (Fig. 2B). Taken together, these results support the
288 notion that *PYL6* repression by ABA rely, at least in part, on the 3'UTR sequence, which
289 contain the miR5628-target sequence.

290 To get further confirmation of miR5628 involvement in *PYL6*-3'UTR cleavage, we
291 used a dual-luciferase-based miRNA sensor system to evaluate whether miR5628 can
292 guide *PYL6* mRNA cleavage *in vivo*. We made three different constructs based on
293 pGreen_dualluc_3'-UTR sensor vector containing either the WT *PYL6* mRNA recognition
294 site of miR5628, or a fully complementarity sequence to the miR5628 sequence
295 (positive control). A negative control consisting of a non-complementary sequence of
296 miR5628 was included (Supplemental Fig. S10C). *Nicotiana benthamiana* leaves were
297 co-transformed with the reporter constructs. The native and positive control
298 constructions showed a tendency to be downregulated in comparison to negative
299 control, further suggesting that miR5628 guides the cleavage of *PYL6* mRNA
300 (Supplemental Fig. S10D). We also generated two transgenic lines overexpressing
301 miR5628 (*oxMIR5628-E4* and *oxMIR5628-E6*) (Supplemental Fig. S11) and analyzed the
302 profile of accumulation of the *PYL6* (5'UTR, CDS and 3'UTR regions) along a time course
303 of ABA treatment (Fig. 2C). In the absence of ABA there is no difference in the abundance
304 of *PYL6* mRNA in the *oxMIR5628-E4* and *oxMIR5628-E6* lines compared to WT (Fig. 2C).
305 However, all regions of *PYL6* transcript are significantly less abundant in the two
306 *oxMIR5628* lines compared to WT in the first 20 min of ABA treatment (Fig. 2C), while
307 after 30 and 60 minutes, no difference in *PYL6* mRNA level was detected between
308 *oxMIR5628* and the WT (Fig. 2C). This result supports the hypothesis that miR5628
309 cleaves *PYL6* transcript and promotes its instability in an ABA-dependent manner.

310 Finally, 5'-RACE analysis was performed with mRNA sampled at 20 min of ABA
311 treatment of oxMIR5628 lines to evaluate the cleavage-activity of miR5628 in these lines
312 (Supplemental Fig S12). 166 cloned 5'-RACE products (52 for WT, 54 for oxMIR5628-E4
313 and 60 for oxMIR5628-E6) were found to match either the miR5628 recognition site in
314 *PYL6* mRNA or downstream to it, but none was localized upstream to miR5628
315 recognition site (Supplemental Fig S12). This result further corroborates that miR5628
316 is involved in *PYL6* transcript decay by promoting *PYL6* transcript cleavage.

317 Based on transcriptional repression by cordycepin we raised the hypothesis that
318 an efficient ABA-induced decay of *PYL6* mRNA rely on an ABA-inducible regulatory
319 factor (Fig. 1E; Supplemental Table S3). MiR5628 emerged as a candidate (Fig. 2A-C),
320 thus, its expression is expected to be regulated by ABA. Indeed, ABA treatment resulted
321 in a transient induction of both *pri-miR5628* and mature *miR5628* (Fig. 2D), reinforcing
322 the regulatory input of miR5628 on *PYL6* transcript stability. Moreover, this transient
323 induction is completely abolished in the double kinase mutant *snrk2d* in response to
324 ABA (Fig. 2E), suggesting that a functional ABA core signaling is required. Additionally,
325 we analyzed the production of *pri-miR5628* and the mature *miR5628* in the miRNAs
326 biogenesis mutants *hyl1-2* and *se-1*. As expected, the *pri-miR5628* accumulated more in
327 both mutants compared to WT in response to ABA, while the mature miR5628 is less
328 abundant in the mutant *hyl1-2* treated with ABA compared to WT and in *se-1* miR5628 is
329 less abundant both in the presence and absence of ABA in relation to WT (Supplemental
330 Fig. S13). These results indicate that ABA controls miR5628 biogenesis.

331

332 **oxMIR5628 affects ABA-induced responses**

333 *PYL6* is more expressed during seed germination suggesting it plays a role in this
334 developmental phase (Klepikova et al., 2016). Thus, we hypothesized that oxMIR5628
335 lines would be hyposensitive to ABA during germination (*i.e.*, radicle emergence). The
336 germination rate of oxMIR5628 genotypes was found to be higher at the concentration
337 of 0.5 and 0.75 μ M of ABA compared to WT, with the largest difference observed at 0.75
338 μ M of ABA (Fig. 3A). At this concentration, the germination rate of oxMIR5628 E4 and E6
339 was 82% and 84%, respectively, while WT was 58% (Fig. 3A). These data confirm that
340 oxMIR5628 lines are hyposensitive to ABA suggesting that miR5628 may impact ABA
341 signaling during germination.

342 The impact of *PYL6* on ABA signaling can also be evaluated through expression
343 analysis of ABA-responsive genes such as *RD29B*, *RD20* and *RAB18* in *oxPYL6* (Fujita et
344 al., 2009; Yoshida et al., 2015). *RD29B*, *RD20* and *RAB18* genes were induced in the
345 *oxPYL6* genotype compared to WT in the absence and presence of ABA (Fig. 3B),
346 suggesting that *PYL6* participates in the control of expression of these ABA readouts
347 genes. We then asked whether miR5628 overexpression could alter ABA-mediated
348 induction of *RD29B*, *RD20* and *RAB18* as would be expected from miR5628-promoted
349 *PYL6* mRNA degradation. In the presence of ABA, no significative difference in the
350 expression of *RD29B*, *RD20*, or *RAB18* between *oxMIR5628* genotypes and WT was
351 detected (Fig. 3C). However, in the absence of ABA, these genes were downregulated in
352 both *oxMIR5628* genotypes compared to WT (Fig. 3C). *In silico* prediction analyzes
353 (psRNA-Target software) showed that *RD29B*, *RD20* and *RAB18* mRNA are not direct
354 target of miR5628. These results suggest that miR5628 indirectly controls the basal
355 expression of ABA signaling readouts possibly by downregulating *PYL6* expression.

356

357 **MiR5628 has emerged in *A. thaliana***

358 We have analyzed whether miR5628 could recognize other *A. thaliana*
359 *PYR/PYL/RCAR* mRNAs. Using the psRNA-Target tool only *PYL6* mRNA was found to be
360 target of miR5628, suggesting a highly specific regulation (Supplemental Fig. S14).
361 Indeed, none of the *PYR/PYL/RCAR* transcript evaluated but *PYL6* was downregulated in
362 the *oxMIR5628* lines compared to WT (Fig. 2C; Supplemental Fig. S15). Then, we have
363 evaluated the evolutionary conservation of miR5628. To this end, BLAST searches were
364 performed for precursor and mature miR5628 sequence similarity against plant genome
365 databases (NCBI). Although a miR5628-related sequence was detected in *Brassica rapa*,
366 the predicted secondary structure of this putative miR5628 precursor was unable to
367 form a hairpin-loop, neither miR5628* and nor expression evidence of this locus was
368 obtained. Finally, we analyzed the global miR5628 expression available in the
369 *Arabidopsis Small RNA Database* (<http://ipf.sustech.edu.cn/pub/asrd/>) (Feng et al.,
370 2020). MiR5628 is poorly expressed (maximum of 3 transcripts per million) as
371 compared to conserved miRNAs (e.g., miR156a-3p with 3,808 transcripts per million)
372 (Supplemental Table S4). The expression of miR5628 is quite comparable to other newly
373 evolved miRNA such as miR5657, miR779.1 and miR865-3p (Supplemental Table S4),
374 which is expected since lineage-specific miRNAs tend to be barely expressed (Fahlgren

375 et al., 2012; Axtell, 2013; Hajieghrari and Farrokhi, 2021). Taken together, these results
376 suggest that miR5628 may have evolved recently in *A. thaliana* lineage.

377
378 **Dynamic of *PYL6* mRNA decay**

379 MiRNAs-mediated mRNA cleavage implies that exosome and XNR4 mediate the
380 degradation of the RISC 5'- and 3'-cleaved fragments, respectively (Chantarachot and
381 Bailey-Serres, 2018). Since miR5628 guides the cleavage of *PYL6* mRNA 3'UTR, a faster
382 decay of this region in comparison to the 5'UTR and coding sequence (CDS) would be
383 expected after ABA treatment. To address this possibility, a short-term kinetic (5 to 60
384 min) of ABA treatment was performed to monitor the rate of decay of different regions
385 of *PYL6* transcript ranging from the 5' to the 3'-end using region-specific primers (Fig.
386 4A). The kinetics degradation profiles of the three different parts of *PYL6* mRNA were
387 found to be similar, suggesting that all parts of *PYL6* transcript are degraded
388 synchronously (Fig. 4A). This conclusion raises the possibility that in addition to
389 miR5628 activity, other mechanisms of mRNA decay are involved in *PYL6* transcript
390 degradation. For instance, decapping has been associated to the control of
391 *PYR/PYL/RCAR* transcript stability and mutants of this machinery are hypersensitive to
392 ABA (Wawer et al., 2018). Additionally, RISC 5'-cleaved fragments of miRNA-targets
393 were suggested to be degraded by the exoribonuclease XRN4 after decapping (Ren et al.,
394 2014). Therefore, we have tested whether decapping followed by XRN4 activity could be
395 involved in the degradation of *PYL6* mRNA.

396 First, we evaluated *PYL6* expression in the *dcp5-1* mutant, which is defective in a
397 component of decapping machinery (Xu and Chua, 2009). *PYL5* was used as a control
398 since it has been shown to be upregulated in *dcp5-1* (Wawer et al., 2018) and, indeed,
399 *PYL5* transcript accumulated more in this mutant as compared to WT after ABA
400 treatment (Fig. 4B). We found that ABA treatment resulted in 4.6-fold increase of *PYL6*
401 mRNA levels in comparison to the WT, which suggests that the decapping machinery is
402 involved in the downregulation of *PYL6* mRNA (Fig. 4B). In addition, *PYL4*, which belong
403 to the same clade as *PYL5* and *PYL6* (Supplemental Fig. S1A), was also less repressed by
404 ABA treatment in *dcp5-1* than in the WT (Fig. 4B). Thus, it is possible that ABA-promoted
405 decapping may be a conserved mechanism for controlling the mRNA stability of these
406 evolutionary related receptors.

407 To evaluated XRN4 involvement in the degradation of RISC 5'-fragment of *PYL6*
408 mRNA, we carried out the quantification of the transcript level corresponding to
409 different parts of *PYL6* transcript (5'UTR, CDS and 3'UTR) in the mutant *xrn4-5* in
410 response to ABA. The amounts of all parts of *PYL6* mRNA were significantly more
411 abundant in the *xrn4-5* mutant in comparison to WT (Fig. 4C). *PYL4* and *PYL5* transcripts
412 were not altered in the mutant *xrn4-5* compared to WT (Supplemental Fig. S16). Since
413 both 5'UTR and CDS regions from *PYL6* transcript are less efficiently reduced in *xrn4-5*,
414 it is possible that XRN4 also participates in the degradation of *PYL6* mRNA from the 5'-
415 end after decapping activity in response to ABA (Fig. 4C). Together, these results suggest
416 5' to 3' mRNA decay pathway is also involved in the degradation of *PYL6* transcript in
417 response to ABA.

418

419 DISCUSSION

420 Negative feedback is a key regulatory scheme in homeostatic processes such as
421 those involved in hormone signaling (Teale et al., 2006; Zhu et al., 2013; Rai et al., 2015;
422 Waters et al., 2017). After the initial increase in hormone levels in response to specific
423 endogenous or exogenous signals, the hormone is detected by receptors and triggers
424 adaptive responses through signaling pathways. These pathways need to be reset to
425 maintain the hormone signaling homeostasis. In response to ABA, the negative feedback
426 is achieved by down- and up-regulation of *PYR/PYL/RCAR* (positive regulators) and
427 *PP2C* (negative regulators) gene expression, respectively (Song et al., 2016) (Fig 1A;
428 Supplemental Fig. S1-S2). Our data highlight the requirement of a functional ABA
429 signaling pathway for efficient ABA-induced downregulation of most *PYR/PYL/RCAR*
430 receptors (Fig. 1C and 1D; Supplemental Fig. S4, S5 and S6). We further show that the
431 control of mRNA decay is an essential step in shaping the ABA-induced repression of
432 *PYL1* (subgroup III) and *PYL4/5/6* (subgroup II) expression (Fig. 1E; Supplemental Fig.
433 S1A and Supplemental Table S3). These receptors have a lower affinity for ABA and
434 were reported to be more active under abiotic stress conditions, when ABA levels are
435 markedly increased (Tischer et al., 2017; Yoshida et al., 2019). Thus, ABA-induced
436 degradation of *PYL1/4/5/6* mRNAs may be part of a strategy to avoid excessive and
437 detrimental ABA responses under stress conditions.

438 The ABA-promoted decay processes of *PYL6* and *PYL1/4/5* transcripts are partly
439 different from each other, since efficient repression of *PYL6* mRNA requires

440 transcription to occur (Supplemental Table S3). This observation suggests that
441 transcription of one causal agent involved in *PYL6* transcript destabilization is induced
442 by the hormone (Fig. 1E; Supplemental Table S3). Therefore, we tested whether the
443 miRNA pathway would be involved in *PYL6* mRNA destabilization in response to ABA.
444 This hypothesis was supported by the impaired repression of *PYL6* mRNA levels by ABA
445 in miRNA pathway mutants (Supplemental Fig. S8). MiR8175, miR5628, miR5021 and
446 miR840-3p were identified as potential miRNAs acting upon *PYL6* transcript (Fig. 2A).
447 Among these, several pieces of evidence indicate that miR5628 is involved in *PYL6*
448 mRNA decay in response to ABA. First, as expected, both *pri-miR5628* and *miR5628* were
449 quickly and transiently induced by ABA (Fig. 2D). This induction coincides with the fast
450 reduction of *PYL6* transcript after ABA addition (2-fold of reduction in 10 minutes; Fig.
451 4A) and requires functional ABA signaling as revealed by the reduced accumulation of
452 miR5628 in *snrk2d* mutant (Fig. 2E). Second, a fusion transcript consisting of GFP and
453 *PYL6* coding sequence, but lacking miRNA5628 target in *PYL6* 3'UTR, was not repressed
454 by ABA (Fig. 2B). Third, the transient expression assay in *N. benthamiana* of a luciferase
455 construct incorporating miR5628 target site in the 3'UTR of LUC gene shown a tendency
456 to reduce the luciferase activity when co-expressed with miR5628 gene (Supplemental
457 Fig. S10D). Fourth, *PYL6* was more repressed during the first 20 minutes of ABA
458 treatment in the miR5628 overexpressing lines (oxMIR5628-E4 and oxMIR5628-E6)
459 compared to WT (Fig 2C). In addition, 5'-RACE products obtained from WT and these
460 over-expressor lines were found to map to the miR5628 recognition site in *PYL6*
461 transcript or downstream to it, but none was found to map upstream (Fig. 2A and
462 Supplemental Fig. S12). Fifth, germination of oxMIR5628 seeds was found to be
463 hyposensitive to ABA (Fig 3A). Thus, it is suggested that miR5628-mediated *PYL6*
464 repression impacts ABA sensitivity at this developmental stage. Finally, XRN4, which is
465 known to degrade RISC 3'-cleaved fragments of miRNA-targets (Souret et al., 2004), was
466 found to be required for efficient ABA-induced decay of *PYL6*-3'UTR mRNA region
467 (Supplemental Fig. S10B). Together, these set of observations support the notion that
468 miR5628 promotes *PYL6* mRNA degradation by promoting its cleavage in an ABA-
469 dependent manner (Fig. 5).

470 MiR5628 is likely to be restricted to *A. thaliana* and is predicted to specifically
471 recognizes *PYL6* mRNA among the 14 *PYR/PYL/RCAR* members (Supplemental Fig. S14
472 and S15). Therefore, we hypothesized that miR5628 is a regulatory novelty that was

473 integrated into the feedback loop of ABA signaling to enhance *PYL6* mRNA decay. This
474 hypothesis would possibly explain the faster and stronger ABA-promoted *PYL6* mRNA
475 decay compared to the others *PYR/PYL/RCAR* transcripts (Fig. 1E, Supplemental Fig. S7
476 and Supplemental Table S3).

477 Intriguingly, miR5628-guided cleavage at the expected canonical position (*i.e.*, 10
478 and 11th nucleotide) was underrepresented in the 5' RACE clones (Supplemental Fig.
479 S12). Such features have been described for other miRNAs (Fahlgren et al., 2007; Lee et
480 al., 2015; Gou et al., 2022; Ren et al., 2022) and, although the underlying reasons are
481 unclear, they would be partly related to peculiarities of newly evolved miRNA (Fahlgren
482 et al., 2012; Axtell, 2013; Hajieghrari and Farrokhi, 2021). In the case of miR5628, some
483 features such as incomplete pairing with its target (Supplemental Fig. S9) and the
484 suboptimal guanine at its 5'-end for AGO1 loading which would affect the stability of
485 miRNA-target duplex, could be responsible for reducing its cleavage activity and
486 contribute to the looser definition of target site cutting (Mi et al., 2008). In addition, it is
487 also possible that the putative secondary structure of *PYL6* mRNA can modulate its
488 recognition by miR5628 (Supplemental Fig. S17)(Zheng et al., 2017).

489 The ABA signaling readouts genes *RD29B*, *RAB18* and *RD20* were upregulated in
490 the *oxPYL6* genotype either in the absence or presence of ABA (Fig. 3B), most likely as a
491 consequence of more receptors triggering ABA signaling. In the oxMIR5628 lines, ABA
492 does not affect the expression of these readout genes as compared to the WT (Figure
493 3C), possibly as a consequence of functional redundancy among PYL/PYR/RCAR
494 receptors (Zhao et al., 2018). In the absence of ABA, these readout genes were
495 downregulated in oxMIR5628 lines (Fig. 3C), yet *PYL6* mRNA levels was not affected
496 (Fig. 2C). The reason for this inconsistency is not clear but may be related to the
497 possibility of miR5628-regulating *PYL6* mRNA translation, since it has been reported
498 that miRNAs which targets 3'-UTR regions, as is the case for miR5628, inhibit the
499 translation of their mRNA targets (Gandikota et al., 2007; Iwakawa and Tomari, 2013).

500 Following miR5628-mediated cleavage of *PYL6* mRNA in response to ABA, we
501 expected that a faster decay of the *PYL6*-3'UTR region in comparison to the 5'UTR and
502 CDS in response to ABA would occur. However, a synchronized pattern of degradation of
503 the 5'UTR, CDS and 3'UTR regions of *PYL6* mRNA after ABA treatment was observed
504 (Fig. 4A), suggesting that, in addition to miR5628 activity, other post-transcriptional
505 regulatory mechanisms would participate in the regulation of *PYL6* transcript decay.

506 Indeed, we provided evidence that the decapping machinery is involved in the ABA-
507 induced reduction of *PYL6* mRNA levels (Fig. 4B). In addition to the degradation of RISC
508 3'-cleaved fragment of *PYL6*-3'UTR, XRN4 is also involved in the degradation of *PYL6*
509 5'UTR and CDS regions (Fig. 4C). These data raise the hypothesis that miR5628-guided
510 *PYL6* mRNA cleavage together with decapping and XRN4 activity would be coupled
511 processes that promote *PYL6* transcript degradation in response to ABA (Fig. 5).

512 Similarly to *PYL6* transcript, the control of mRNA decay of *PYL4/5* receptors, at
513 least in part, rely on decapping activity, since these transcripts were shown to be less
514 responsive to ABA in the decapping *dcp5-1* mutant (Fig. 4B). This result is in line with
515 the observation that the mRNA of these two receptors and of *PYL6* are targets of
516 VARICOSE, another component of decapping machinery (Sorenson et al., 2018). Since
517 *PYL4/5/6* are part of the same clade in subgroup III (Supplemental Fig. S1A), we suggest
518 that the involvement of decapping in the control of the stability of these ABA receptors
519 transcripts is an ancestral regulatory feature.

520 The control of PYR/PYL/RCAR protein stability is another aspect of the dynamic
521 of regulation of the ABA signaling. Most PYR/PYL/RCAR receptors tend to be
522 ubiquitinated and degraded by the 26S proteasome in the absence of ABA and stabilized
523 in the presence of ABA (Irigoyen et al., 2014; Chen et al., 2018; Li et al., 2018). This
524 regulation favors the establishment of ABA-induced gene expression programs. Fast
525 ABA-induced repression of *PYL1*, *PYL4*, *PYL5* and *PYL6* transcripts levels through, at
526 least in part, the control of mRNA stability, would counterbalance receptors stabilization
527 and contribute to limit *de novo* synthesis of receptors and, thus, constrain ABA-
528 responses. Hence, the balance between PYR/PYL/RCAR protein stability and the level of
529 the corresponding mRNA would define the extent of ABA signalization and is likely an
530 important facet in the homeostasis of ABA signaling.

531

532 MATERIAL AND METHODS

533 Plant material and growth conditions

534 Five milligrams of seeds were surface-sterilized and added to 10 mL of half-
535 strength liquid Murashige and Skoog medium (MS/2) adjusted to 0.3% of Glucose (Glc)
536 (w/v). After stratification at 4°C for three days, seedlings were grown under constant
537 light (Photosynthetically Active Radiation/PAR of 100 $\mu\text{mol m}^{-2}\text{s}^{-1}$) at 21°C for 6 days
538 under constant agitation (60 rpm). On the sixth day, samples were treated with 1 μM

539 ABA (final concentration) for different times. Five biological replicates per treatment
540 were used. The following mutant lines in the Col-0 background were used: *abi1-1*
541 (Umezawa et al., 2009), *abi4-1* (Finkelstein, 1994), *snrk2d* (Fujii et al., 2007), *se-1*, *hyl1-2*
542 (Vazquez et al., 2004), *ago1-25* (Morel et al., 2002), *dcp5-1* (Xu and Chua, 2009) and
543 *xrn4-5* (Souret et al., 2004). Seeds of Col-0 background containing the fusion between
544 the coding sequence of the Green Fluorescent Protein (GFP) and of PYL6 under the
545 control of the *Cauliflower Mosaic Virus (CaMV)* 35S promoter (*oxPYL6*) were described in
546 Belda-Palazon et al. (2016).

547 *Nicotiana benthamiana* plants were grown at 22°C under relative humidity 65%
548 and 16h/8h (light/dark) conditions on plastic cups containing peat:vermiculite (1:1).
549 Plants at six weeks after germination were used for Agroinfiltration.

550

551 **Seed germination analysis**

552 Surface-sterilized seeds were sown on half-strength solid MS adjusted to 0.3% Glc
553 (w/v) and grown under continuous light (PAR of 100 $\mu\text{mol m}^{-2}\text{s}^{-1}$). Seed germination
554 rate (%) corresponds to the number of seeds that germinated each day for the total of
555 seeds germinated at the sixth day. We apply Tukey and Scott-Knott test to evaluate
556 significant differences in the germination rate.

557

558 **RNA isolation and gene expression analysis**

559 Total RNA extraction, cDNA synthesis and real-time quantitative reverse
560 transcription polymerase chain reaction (RT-qPCR) were conducted as previously
561 described (Matiolli et al., 2011; Duarte et al., 2013). Relative quantification levels were
562 calculated by the $2^{-\Delta\Delta\text{CT}}$ formula. To quantify different parts of *PYL6* and *GFP* transcripts
563 in WT and *oxPYL6* genotypes the formula $2^{(\text{Ct target gene} - \text{Ct reference genes}) \times 100}$ was used. The
564 reference genes were *PDF2* (AT1G13320) and *EF-1 α* (AT5G60390) (Czechowski et al.,
565 2005). Stem-loop RT-qPCR miRNA assay was carried out for the quantification of mature
566 miRNA (Varkonyi-Gasic et al., 2007). Differences in gene expression were considered
567 significant for fold changes $\geq |1.5|$ between treated and control samples and for $p < 0.05$
568 according to two-tailed Student's t test. The primer sequences for RT-qPCR are shown in
569 Supplemental Table S1.

570

571 **Staurosporine and Cordycepin treatments**

572 Five days-old seedlings were treated for 24 h with 10 μ M staurosporine (stock
573 solution 100 mM in dimethylsulfoxide; Sigma S5921). On the sixth day, the seedlings
574 were treated with 1 μ M ABA for 1 hour (h). Control samples were treated with DMSO.

575 Transcription inhibition was performed with 100 μ M cordycepin (3-
576 deoxyadenosine; Sigma C3394) from a 100 mM stock aqueous solution. To evaluate
577 ABA-mediated control of mRNA stability we proceed according describe by Matioli et al.
578 (2011).

579

580 **5'-RACE analysis**

581 5'RACE was performed using the GeneRacer kit (Invitrogen) according to the
582 manufacturer's recommendations. Five micrograms of total RNA were ligated to the
583 RNA GeneRacer oligo adapter and subjected to reverse transcription utilizing Improm-II
584 Reverse Transcriptase kit (Promega). The cDNA was used for amplification of cleaved
585 *PYL6* fragments, using a forward primer specific for the sequence of the GeneRacer RNA
586 oligo adapter and a reverse primer specific for the *PYL6* mRNA (Supplemental Table S2).
587 PCR products were then used as a template for a NESTED PCR with internal *PYL6*
588 specific primers (Supplemental Table S2). After amplification, 5'RACE products were
589 gel-purified and cloned in pGem®-T Easy vector (Promega). Independent clones were
590 randomly chosen and sequenced by Sanger sequencing method.

591

592 **DNA constructions**

593 Plasmids used in this study were constructed by modifying the pGreen dual-Luc
594 3'-UTR sensor plasmid by double digested with *Age*I and *Avr*II restriction enzymes, as
595 early described (Liu et al., 2014). T4 DNA ligase-mediated insertion of *PYL6* target
596 sequence (WT sequence), miR5628 perfect match (positive control) or non-
597 complementary sequence of miR5628 (negative control) into the 3'-UTR pGreen dual-
598 Luc plasmid was performed and Sanger sequenced. Versions of miR5628 targets sites
599 were obtained by annealing two complementary primers (Supplemental Table S2). For
600 precursor of miR5628 of *A. thaliana*, we designed forward and reverse primers 180 and
601 122 nucleotides up and downstream to the precursor sequence of miR5628, respectively
602 (Supplemental Table S2). Products of PCR amplified were sub-cloned into pENTR™
603 Directional TOPO® and further Sanger sequenced followed by cloning into the Gateway
604 pK7WG2.0.

605

606 **Agroinfiltration and Dual-luciferase assay**

607 Plasmids were introduced by electroporation into *Agrobacterium tumefaciens*
608 strain GV3101 (harboring pSOUP) and plated on LB agar broth containing rifampicin (25
609 $\mu\text{g/mL}$), gentamicin (25 $\mu\text{g/mL}$) and kanamycin (50 $\mu\text{g/mL}$) selection. Primary
610 inoculations were prepared by inoculating a single colony and grown overnight at 28°C
611 in a shaking incubator. Working cultures were harvested by centrifugation at room
612 temperature at 3000 rpm for 10 min. Cell pellets were resuspended in 2 mL of room
613 temperature infiltration media (88.5 mL water, 1 mL 1M MgCl₂, 10 mL 100 mM MES, 75
614 μL 200 mM acetosyringone) and stored in the dark at room temperature for 4 h. The
615 OD₆₀₀ were adjusted to about 0.5. In three 15-mL falcon tubes it was mixed OD₆₀₀-
616 adjusted sensor and p35S::MIR5628 culture per tube at 1:1 ratio. Three expanded leaves
617 per plant were infiltrated by applying pressure on the abaxial surface of the leaf with a
618 1-mL syringe with well-mixed *Agrobacterium* suspension.

619 After 3 days of agroinfiltration treatment it was punched two leaf discs from each
620 leaf and placed into 1.5 mL eppendorf tube. Samples were frozen immediately into liquid
621 nitrogen and grinded. Fine power was resuspended into the ice-chilled lysis buffer (PLB)
622 and shacked on vortex to completely resuspend the tissue powder in the solution.
623 Resuspended samples were centrifuged at 14000 rpm, 4°C, for 1 min to pellet cell
624 debris. It was loaded 20 μL of the supernatant from each sample into designated
625 position on the 96-well plate. The substrate solution LARII was prepared for firefly
626 Luciferase, and the substrate solution Stop&Glo was used for Renilla. The analysis was
627 performed on GloMax 96 Microplate Luminometer (Promega), and the F-Luc/R-Luc
628 ratio was calculated for all samples and technical replicates.

629

630 **Generation of Transgenic lines**

631 To make oxMIR5628 lines, the vector pK7WG2.0, containing the 35S:MIR5628
632 fusion, were introduced by electroporation into *A. tumefaciens* strain GV3101 and plated
633 on LB agar broth containing rifampicin (25 $\mu\text{g/mL}$) and kanamycin (50 $\mu\text{g/mL}$)
634 selection. Then, Arabidopsis plants (Col-0 background) were transformed according
635 floral dip method. Transformants were selected by their kanamycin (50 $\mu\text{g/mL}$)
636 resistance and validated by PCR. Homozygous lines (oxMIR5628) were used for
637 experiments.

638

639 **Bioinformatics analysis**

640 The software psRNA-target was used to identify putative miRNAs that can
641 recognize *PYL6* transcript (<http://plantgrn.noble.org/psRNATarget/home>) (Dai et al.,
642 2018). Analysis of miRNA conservation was carried out using BLAST. Both precursor
643 (pre-miR5628) and mature miR5628 sequences were used as query to search for
644 homologs in the genomes of the vegetal kingdom available at the National Center for
645 Biotechnology Information (NCBI) (<https://www.ncbi.nlm.nih.gov/>). Blast parameters
646 were adjusted as follows: expect values were set at 1000; high similar sequences were
647 chosen as the sequence filter; the number of descriptions and alignments was raised to
648 1000 and the default word-match size between the query and database sequences was
649 seven. The ability of sequences similar to pre-miR5628 to form stem-loop structure *in*
650 *silico* was evaluated using the RNAfold web server (<http://rna.tbi.univie.ac.at/>) (Gruber
651 et al., 2008) and their expression was verified searching transcriptomes data available in
652 the Sequence Read Archive (RSA) at the NCBI and. We analyzed the global miR5628
653 expression available in the *Arabidopsis Small RNA Database*
654 (<http://ipf.sustech.edu.cn/pub/asrd/>) (Feng et al., 2020).

655 Amino acid sequences of the 14 *A. thaliana* PYR/PYL/RCAR were retrieved from
656 the TAIR10 database (<https://www.arabidopsis.org/>). These sequences were used to
657 infer the phylogenetic relationship of these proteins using Neighbor-Joining method and
658 draw the corresponding tree of similarity using MEGA7 program (Kumar et al., 2016).

659

660 **ACKNOWLEDGEMENTS**

661 The authors are grateful to Hervé Vaucheret, Baena-González, Jian-Kang Zhu and
662 Pedro Rodriguez for providing seeds of the different genotypes used in this work. This
663 work was funded by Fundação de Amparo à Pesquisa do Estado de São Paulo (FAPESP):
664 Vincentz, M (grant 2015/25838-2), Vieira JGP (grant 2016/0498-7 and 2019/25696-4)
665 and Duarte, GT (grant 12/22125-7).

666

667 **SUPPLEMENTAL DATA**

668 **Supplemental Table S1:** Sequence of oligonucleotides used for RT-qPCR analysis.

669 **Supplemental Table S2:** Sequence of oligonucleotides used for 5'RACE and Dual-
670 luciferase analyses.

671 **Supplemental Table S3:** ABA-induced changes in the mRNA stability of
672 PYR/PYL/RCAR.

673 **Supplemental Table S4:** Global expression of miR5628 in comparison to newly evolved
674 and conserved miRNAs in *Arabidopsis thaliana*.

675 **Supplemental Figure S1:** Effect of ABA treatment on gene expression of ABA core
676 signaling components.

677 **Supplemental Figure S2:** mRNA profiles of ABA core signaling pathway genes in
678 response to long-term treatment with ABA.

679 **Supplemental Figure S3:** Changes in the expression profile of ABA core signaling
680 pathway genes in response to a short ABA treatment.

681 **Supplemental Figure S4:** Downregulation of *PYR/PYL/RCAR* gene expression requires
682 a functional ABA core signaling pathway.

683 **Supplemental Figure S5:** Global kinase inhibition by staurosporine affects the
684 expression of *PYR/PYL/RCAR* and clade A *PP2C* genes in response to ABA.

685 **Supplemental Figure S6:** Kinases SnRK2 from subclass III are involved in the
686 downregulation of *PYR/PYL/RCAR* gene expression in response to ABA.

687 **Supplemental Figure S7:** Impact of ABA on the *PYL1*, *PYL2* and *PYL8* mRNA stability.

688 **Supplemental Figure S8:** Involvement of miRNA pathway in the control of *PYL6*
689 expression in response to ABA.

690 **Supplemental Figure S9:** Schematic representation of *PYL6* mRNA and the position of
691 the putative miR8175, miR5628, miR5021 and miR840-3p target sequences.

692 **Supplemental Figure S10:** Analyses of cleavage of *PYL6* mRNA by miR5628.

693 **Supplemental Figure S11:** Lineages oxMIR5628-E4 and oxMIR5628-E6 overexpressed
694 both the primary miR5628 sequence (*pri-miR5628*) and mature miR5628 sequence
695 (*miR5628*).

696 **Supplemental Figure S12:** Schematic representation of 5'RACE cloned sequences of
697 *PYL6* mRNA upon 20 minutes of ABA treatment in the oxMIR5628 (E4 and E6) lineages
698 and Col-0.

699 **Supplemental Figure S13:** MiR5628 biogenesis is controlled by ABA.

700 **Supplemental Figure S14:** Divergence of the miR5628 recognition sequence among the
701 14 *A. thaliana* ABA receptors.

702 **Supplemental Figure S15:** Overexpression of miR5628 do not impact the expression of
703 *PYL1*, *PYL2*, *PYL4*, *PYL5* and *PYL8*.

704 **Supplemental Figure S16:** Analysis of *PYL4* and *PYL5* mRNA accumulation in wild type
705 (WT) and *xrn4-5* in response to ABA treatment.

706 **Supplemental Figure S17:** Predicted *PYL6* mRNA 3'-UTR secondary structure includes
707 miR5628 target site.

708

709 **FIGURES AND LEGENDS**

710 **Figure 1: Regulation of the expression of ABA core signaling pathway genes by**
711 **ABA.**

712 (A) mRNA profile of members of the ABA core signaling pathway in response to long-
713 term ABA treatment. One member of each subgroup of PYR/PYL/RCAR and three
714 members of clade A PP2Cs (Supplemental Fig. S1A) are represented, along with subclass
715 III SnRK2 members. An expanded analysis with *PYR/PYL/RCAR* and *PP2C* genes is given
716 in Supplemental Fig. S2. Seedlings were treated with 1 μ M ABA for up to 16 hours.

717 (B) mRNA profile of members of the ABA core signaling pathway in response to
718 transient ABA-treatment. Seedlings were treated with 1 μ M ABA for 30 min, then ABA
719 was removed from the medium. Sampling was performed before the treatment (0 h), at
720 the end of the 30 min (in the gray box) of ABA-treatment, and at different time points
721 after hormone removal. An expanded analysis with *PYR/PYL/RCAR* and *PP2C* genes is
722 given in Supplemental Fig. S3.

723 In panels A and B "a" means significant difference between each time point vs the
724 untreated control and "b" each time point vs. the previous one. Responses were
725 significantly different for fold changes in mRNA levels $\geq |1.5|$ and $p < 0.05$, according to
726 Student's t-test. The color of the letter refers to the gene evaluated.

727 (C) The negative feedback regulation of the ABA core signaling pathway requires ABA-
728 signalization. Wild type (WT) and *abi1-1* seedlings were treated with 1 μ M ABA for 1
729 hour before sampling. Expression of the ABA-induced *Rd29B* gene was used as positive
730 control of ABA-promoted responses. *PYL6* response is shown and a complete analysis of
731 the expression of six other representative ABA receptors is provided in Supplemental
732 Fig. S4. The expression levels are given in comparison to the untreated WT.

733 (D) Kinases SnRK2 are involved in the negative feedback of *PYR/PYL/RCAR* genes in
734 response to ABA. WT and the double kinase mutant *snrk2.2/snr2.3* (*snrk2d*) seedlings
735 were treated with 1 μ M ABA for 1 hour before sampling. Expression of the ABA-induced
736 *Rd29B* gene was used as positive control of ABA-promoted responses. *PYL6* response is

737 shown and a complete analysis of the expression of the six other representative ABA
738 receptors is provided in Supplemental Fig. S6. The expression levels are given in
739 comparison to the untreated WT.

740 (E) ABA regulates *PYL1*, *PYL4*, *PYL5* and *PYL6* mRNA stability. To evaluate ABA-
741 mediated control of mRNA stability, seedlings were pre-treated for 1 h with 100 μ M
742 cordycepin (Cord) to inhibit transcription, followed by the addition of ABA 1 μ M (Cord +
743 ABA). After cordycepin pre-treatment sampling was performed at 20, 40 and 60 minutes
744 with and without ABA. Relative expression values in Cord + ABA condition that are
745 lower than the respective Cord treatment alone indicate that the stability of the
746 transcript was decreased in response to ABA. A complete analysis of the mRNA stability
747 of representative *PYR/PYL/RCAR* genes is given in Supplemental Table S3.

748 For all experiments, values are the mean of five biological replicates \pm standard
749 deviation. Responses were significantly different for fold changes in mRNA levels $\geq |1.5|$
750 and $p < 0.05$, according to Student's t-test (* < 0.05 ; ** < 0.005 ; *** < 0.0005).

751

752 **Figure 2: MiR5628 promotes cleavage of *PYL6* mRNA in response to ABA.**

753 (A) Schematic representation of *PYL6* mRNA with the putative miR8175, miR5628,
754 miR5021 and miR840-3p and the position of their binding sites in *PYL6* mRNA. 5'-RACE
755 analysis of *PYL6* mRNA cleavage by miR5628 in Col-0. Forty-seven cloned sequences (in
756 black) mapped to the miR5628 recognition site (position 784-804 bp of *PYL6* mRNA) or
757 downstream of it in the 3'UTR sequence (blue). The number of occurrences of each
758 sequence is indicated.

759 (B) The 3'UTR of *PYL6* transcript is required for proper control of its stability in
760 response to ABA. The relative amounts of the CDS and 3'UTR sequences of *PYL6* mRNA
761 was quantified in wild type (WT) and in a transgenic line expressing the 35S:GFP:PYL6
762 (Col-0 background), which lacks the *PYL6* 3'UTR region (*oxPYL6*). Amplification of *GFP*
763 sequence allows to quantify specifically the *oxPYL6* fusion. Fourteen days old seedlings
764 grown under continuous light were treated with 1 μ M ABA for 30 min. This analyze is
765 representative of three independent experiments.

766 (C) miR5628 participates in the degradation of *PYL6* transcript in response to ABA. The
767 amount of *PYL6*-5'UTR, CDS and 3'UTR sequences (primers positions are shown in panel
768 A) was quantified at different time points of a 60 min treatment with 1 μ M ABA in

769 samples of oxMIR5628 (E4 and E6) and WT seedlings. Relative expression values of each
770 genotype were obtained in comparison to the untreated WT. This analyze is
771 representative of two independent experiments.

772 **(D)** ABA transiently induces both the *pri-miR5628* and the mature *miR5628*. Col-0
773 seedlings were treated with 1 μ M ABA and sampling was performed before (0 min) and
774 at 5, 10, 20, 30 and 60 minutes after ABA application. Relative expression values were
775 obtained in comparison to the untreated condition (time point of 0 min). This analyze is
776 representative of four independent experiments.

777 **(E)** A functional ABA signaling is required to transient induction of *pri-miR5628* and the
778 mature *miR5628* in response to ABA. WT and the double kinase mutant *snrk2d*
779 (*snrk2.2/snr2.3*) seedlings were treated with 1 μ M ABA and sampling was performed
780 before (0 min), at 5 and 60 minutes after ABA application. The relative expression levels
781 are given in comparison to the untreated WT.

782 In panels B, C, D and E, values are the means of five biological replicates \pm standard
783 deviation. RT-qPCR was carried out to gene quantification. Responses were significantly
784 different for fold changes in mRNA levels \geq |1.5| and $p < 0.05$, according to Student's t-
785 test (* < 0.05 ; ** < 0.005 ; *** < 0.0005).

786

787 **Figure 3: miR5628 impacts ABA signaling.**

788 **(A)** oxMIR5628 lines are hyposensitive to ABA during germination. The germination
789 rate of WT, oxMIR5628 lines, *abi4-1* and *dcp5-1* genotypes were evaluated in continuous
790 light on solid (0.25% of agar) MS/2 medium along a range of ABA concentrations (0,
791 0.25, 0.5, 0.75 e 1 μ M of ABA). The data represent the average of three biological
792 replicates (three plates) with at least 30 seeds for each genotype. Seeds germination was
793 monitored during six days after exposure to light. The seed germination rate (%)
794 corresponds to the number of seeds that germinated each day for the total of seeds
795 germinated at the sixth day. The graphic represents the differences observed at the
796 second day. The mutants *abi4-1* and *dcp5-1* were used as control for ABA-hypo and -
797 hypersensitive phenotypes, respectively. Responses were significantly different for
798 changes in the germination rate according to Tukey and Scott-Knott test, which is
799 represented by the letters "a" (statistical difference in relation to WT), "b" (statistical

800 difference in relation to *abi4-1*) and “c” (statistical difference in relation to *dcp5-1*). This
801 analyze is representative of two independent experiments.

802 **(B)** ABA signaling readout genes (*RD29B*, *RAB18* and *RD20*) are upregulated in the
803 *oxPYL6* genotype both in the presence and absence of ABA. WT and *oxPYL6* seedlings
804 were treated with 1 μ M ABA for 1 hour before sampling. Relative expression values of
805 each genotype were obtained in comparison to the untreated WT. This analyze is
806 representative of three independent experiments.

807 **C)** ABA signaling readout genes (*RD29B*, *RAB18* and *RD20*) are downregulated in the
808 *oxMIR5628* lines. WT and *oxMIR5628* (E4 and E6) seedlings were treated with 1 μ M
809 ABA for 1 hour before sampling. Relative expression values of each genotype were
810 obtained in comparison to the untreated WT. This analyze is representative of three
811 independent experiments.

812 In panels B and C, values are the means of five biological replicates \pm standard deviation.
813 RT-qPCR was carried out to gene quantification. Responses were considered to be
814 significantly different for fold changes in mRNA levels $\geq |1.5|$ and $p < 0.05$, according to
815 Student's t-test (* < 0.05 ; ** < 0.005 ; *** < 0.0005).

816

817 **Figure 4: 5'-3' mRNA decay pathway is involved in the control of *PYL6* mRNA
818 accumulation in response to ABA.**

819 **(A)** Schematic representation of *PYL6* mRNA with the 5'- and 3'-UTRs and coding
820 sequence (CDS) regions, and miR5628 target site. The position of primer pairs that were
821 used to measure the level of mRNA corresponding to different parts of *PYL6* transcript
822 are shown. The different regions of *PYL6* were quantified by RT-qPCR along a time
823 course of ABA treatment. Seedlings were grown for six days and were treated with 1 μ M
824 ABA. Sampling was performed before (0 min) and at 5, 10, 20, 30 and 60 min after ABA
825 application. This analyze is representative of three independent experiments.

826 **(B)** *PYL4*, *PYL5* and *PYL6* transcripts profiles were compared between the mutant *dcp5-1*,
827 which is defective in decapping activity, and the wild type (WT) in response to ABA
828 treatment.

829 **(C)** Accumulation of 5'UTR, CDS and 3'UTR regions of *PYL6* mRNA compared between
830 *xrn4-5* mutant and WT in response to ABA. This analysis represents three independent
831 experiments.

832 In panels B and C, seedlings were treated with 1 μ M ABA for 1 hour before sampling.
833 Values are the means of five biological replicates \pm standard deviation. The relative
834 levels of transcripts were obtained in comparison to the untreated WT. Responses were
835 significantly different for fold changes in mRNA levels \geq |1.5| and $p < 0.05$, according to
836 Student's t-test (* < 0.05 ; ** < 0.005 ; *** < 0.0005).

837

838 **Figure 5: Model of the control of ABA signalization through repression of**
839 ***PYR/PYL/RCAR* genes.**

840 Abiotic stress conditions such as drought, increase the endogenous level of ABA, which
841 is perceived by PYR/PYL/RCAR receptors. The ABA-receptor complex sequesters Clade
842 A PP2C phosphatases, releasing SnRK2 kinases from their negative regulation. These
843 SnRK2s phosphorylate several proteins in order to activate the gene expression
844 program of ABA responses. Part of these ABA responses are involved in the
845 transcriptional repression of *PYL1/2/4/5/6* and *PYL8* genes. In addition, ABA
846 accelerates the decay of *PYL1/4/5/6* transcripts. The ABA core signaling pathway
847 induces miR5628 expression, which in turn is processed and loaded onto AGO1. AGO1-
848 miR5628 complex promotes the cleavage of *PYL6* mRNA at the 3'UTR region, and XRN4
849 promotes the degradation of the RISC 3'-cleaved fragment of *PYL6*. Additionally, the
850 dynamic of *PYL6* mRNA decay may involve the participation of 5' to 3' mRNA decay
851 pathway, where RISC 5'-cleaved fragment of *PYL6* transcripts would undergo decapping
852 followed by XRN4-mediated degradation. Decapping may also contribute to destabilize
853 *PYL4* and *PYL5* transcripts, which are phylogenetically close to *PYL6*. The repression of
854 *PYR/PYL/RCAR* genes expression is a mean to limit de novo synthesis of receptors,
855 controlling the extension of ABA responses and participating in the resetting of the ABA
856 signaling. In addition, it might be possible that miR5628 would regulate *PYL6* mRNA
857 translation.

858

859 **LITERATURE CITED**

860 **Axtell MJ** (2013) Classification and comparison of small RNAs from plants. *Annu Rev*
861 *Plant Biol* **64**: 137–159
862 **Barrera-Rojas CH, Otoni WC, Nogueira FTS** (2021) Shaping the root system: the
863 interplay between miRNA regulatory hubs and phytohormones. *J Exp Bot* **72**:
864 6822–6835
865 **Belda-Palazon B, Rodriguez L, Fernandez MA, Castillo M-C, Anderson EA, Gao C,**

867 **González-Guzmán M, Peirats-Llobet M, Zhao Q, De Winne N, et al** (2016)
868 FYVE1/FREE1 Interacts with the PYL4 ABA Receptor and Mediates its Delivery to
869 the Vacuolar Degradation Pathway. *Plant Cell* **28**: tpc.00178.2016

870 **Chantarachot T, Bailey-Serres J** (2018) Polysomes, Stress Granules, and Processing
871 Bodies: A Dynamic Triumvirate Controlling Cytoplasmic mRNA Fate and Function.
872 *Plant Physiol* **176**: 254–269

873 **Chen H-H, Qu L, Xu Z-H, Zhu J-K, Xue H-W** (2018) EL1-like Casein Kinases Suppress
874 ABA Signaling and Responses by Phosphorylating and Destabilizing the ABA
875 Receptors PYR/PYLs in Arabidopsis. *Mol Plant* **11**: 706–719

876 **Chu LH, Jeng ST** (2002) Multiple transduction pathways regulate the 35S promoter with
877 an ABA responsive element. *Plant Sci* **163**: 23–32

878 **Czechowski T, Stitt M, Altmann T, Udvardi MK, Scheible W-R** (2005) Genome-wide
879 identification and testing of superior reference genes for transcript normalization
880 in Arabidopsis. *Plant Physiol* **139**: 5–17

881 **Dai X, Zhuang Z, Zhao PX** (2018) psRNATarget: a plant small RNA target analysis
882 server (2017 release). *Nucleic Acids Res* **46**: W49–W54

883 **Davière J-M, Achard P** (2013) Gibberellin signaling in plants. *Development* **140**: 1147–
884 1151

885 **Duarte GT, Matiolli CC, Pant BD, Schlereth A, Scheible W-RW-R, Stitt M, Vicentini R,**
886 **Vincentz M** (2013) Involvement of microRNA-related regulatory pathways in the
887 glucose-mediated control of Arabidopsis early seedling development. *J Exp Bot* **64**:
888 4301–4312

889 **Fahlgren N, Howell MD, Kasschau KD, Chapman EJ, Sullivan CM, Cumbie JS, Givan
890 SA, Law TF, Grant SR, Dangl JL, et al** (2007) High-Throughput Sequencing of
891 Arabidopsis microRNAs: Evidence for Frequent Birth and Death of MIRNA Genes.
892 *PLoS One* **2**: e219

893 **Fahlgren N, Jogdeo S, Kasschau KD, Sullivan CM, Chapman EJ, Laubinger S, Smith
894 LM, Dasenko M, Givan SA, Weigel D, et al** (2012) MicroRNA Gene Evolution in
895 *Arabidopsis lyrata* and *Arabidopsis thaliana*. *Plant Cell* **22**: 1074–1089

896 **Feng L, Zhang F, Zhang H, Zhao Y, Meyers BC, Zhai J** (2020) An Online Database for
897 Exploring Over 2,000 Arabidopsis Small RNA Libraries. *Plant Physiol* **182**: 685–691

898 **Finkelstein RR** (1994) Mutations at two new Arabidopsis ABA response loci are similar
899 to the *abi3* mutations. *Plant J* **5**: 765–771

900 **Fujii H, Verslues PE, Zhu JK** (2007) Identification of Two Protein Kinases Required for
901 Abscisic Acid Regulation of Seed Germination, Root Growth, and Gene Expression in
902 Arabidopsis. *Plant Cell* **19**: 485–494

903 **Fujita Y, Nakashima K, Yoshida T, Katagiri T, Kidokoro S, Kanamori N, Umezawa T,**
904 **Fujita M, Maruyama K, Ishiyama K, et al** (2009) Three SnRK2 Protein Kinases are
905 the Main Positive Regulators of Abscisic Acid Signaling in Response to Water Stress
906 in Arabidopsis. *Plant Cell Physiol* **50**: 2123–2132

907 **Gandikota M, Birkenbihl RP, Höhmann S, Cardon GH, Saedler H, Huijser P** (2007)
908 The miRNA156/157 recognition element in the 3' UTR of the Arabidopsis SBP box
909 gene SPL3 prevents early flowering by translational inhibition in seedlings. *Plant J*
910 **49**: 683–693

911 **Gou X, Zhong C, Zhang P, Mi L, Li Y, Lu W, Zheng J, Xu J, Meng Y, Shan W** (2022)
912 miR398b and AtC2GnT form a negative feedback loop to regulate Arabidopsis
913 thaliana resistance against Phytophthora parasitica. *Plant J* **111**: 360–373

914 **Gruber AR, Lorenz R, Bernhart SH, Neubock R, Hofacker IL** (2008) The Vienna RNA
915 Websuite. *Nucleic Acids Res* **36**: W70–W74

916 **Hajieghrari B, Farrokhi N** (2021) Investigation on the Conserved MicroRNA Genes in
917 Higher Plants. *Plant Mol Biol Report* **39**: 10–23

918 **Irigoyen ML, Iniesto E, Rodriguez L, Puga MI, Yanagawa Y, Pick E, Strickland E, Paz-**
919 **Ares J, Wei N, De Jaeger G, et al** (2014) Targeted degradation of abscisic acid
920 receptors is mediated by the ubiquitin ligase substrate adaptor DDA1 in
921 *Arabidopsis*. *Plant Cell* **26**: 712–28

922 **Iwakawa H, oki, Tomari Y** (2013) Molecular Insights into microRNA-Mediated
923 Translational Repression in Plants. *Mol Cell* **52**: 591–601

924 **Kavi Kishor PB, Tiozon RN, Fernie AR, Sreenivasulu N** (2022) Abscisic acid and its
925 role in the modulation of plant growth, development, and yield stability. *Trends
926 Plant Sci* **27**: 1283–1295

927 **Kieber JJ, Schaller GE** (2018) Cytokinin signaling in plant development. *Development*
928 **145**: dev149344

929 **Klepikova A V, Kasianov AS, Gerasimov ES, Logacheva MD, Penin AA** (2016) A high
930 resolution map of the *Arabidopsis thaliana* developmental transcriptome based on
931 RNA-seq profiling. *Plant J* **88**: 1058–1070

932 **Kumar S, Stecher G, Tamura K** (2016) MEGA7: Molecular Evolutionary Genetics
933 Analysis Version 7.0 for Bigger Datasets. *Mol Biol Evol* **33**: 1870–1874

934 **Lee HJ, Park YJ, Kwak KJ, Kim D, Park JH, Lim JY, Shin C, Yang KY, Kang H** (2015)
935 MicroRNA844-guided downregulation of cytidinephosphate diacylglycerol
936 Synthase3 (CDS3) mRNA affects the response of *arabidopsis thaliana* to bacteria
937 and fungi. *Mol Plant-Microbe Interact* **28**: 892–900

938 **Li D, Zhang L, Li X, Kong X, Wang X, Li Y, Liu Z, Wang J, Li X, Yang Y** (2018) AtRAE1 is
939 involved in degradation of ABA receptor RCAR1 and negatively regulates ABA
940 signalling in *Arabidopsis*. *Plant Cell Environ* **41**: 231–244

941 **Liu Q, Wang F, Axtell MJ** (2014) Analysis of complementarity requirements for plant
942 microRNA targeting using a *Nicotiana benthamiana* quantitative transient assay.
943 *Plant Cell* **26**: 741–53

944 **Ma Y, Szostkiewicz I, Korte A, Moes D, Yang Y, Christmann A, Grill E** (2009)
945 Regulators of PP2C Phosphatase Activity Function as Abscisic Acid Sensors. *Science*
946 (80-) **324**: 1064–1069

947 **Matiolli CC, Tomaz JP, Duarte GT, Prado FM, Del Bem LEV, Silveira AB, Gauer L,
948 Corrêa LGG, Drumond RD, Viana AJC, et al** (2011) The *Arabidopsis* bZIP gene
949 AtbZIP63 is a sensitive integrator of transient abscisic acid and glucose signals.
950 *Plant Physiol* **157**: 692–705

951 **Mi S, Cai T, Hu Y, Chen Y, Hedges E, Ni F, Wu L, Li S, Zhou H, Long C, et al** (2008)
952 Sorting of small RNAs into *Arabidopsis* argonaute complexes is directed by the 5'
953 terminal nucleotide. *Cell* **133**: 116–127

954 **Morel J-BJ-B, Godon C, Mourrain P, Béclin C, Boutet S, Feuerbach F, Proux F,
955 Vaucheret H** (2002) Fertile hypomorphic ARGONAUTE (ago1) mutants impaired in
956 post-transcriptional gene silencing and virus resistance. *Plant Cell* **14**: 629–39

957 **Mugridge JS, Coller J, Gross JD** (2018) Structural and molecular mechanisms for the
958 control of eukaryotic 5'-3' mRNA decay. *Nat Struct Mol Biol* **25**: 1077–1085

959 **Park S, Fung P, Nishimura N, Jensen DR, Fujii H, Zhao Y, Lumba S, Santiago J,
960 Rodrigues A, Chow TF, et al** (2009) Abscisic Acid Inhibits Type 2C Protein
961 Phosphatases via the PYR/PYL Family of START Proteins. *Science* (80-) **324**: 1068–
962 1069

963 **Rai MI, Wang X, Thibault DM, Kim HJ, Bombyk MM, Binder BM, Shakeel SN,
964 Schaller GE** (2015) The ARGOS gene family functions in a negative feedback loop to

965 desensitize plants to ethylene. *BMC Plant Biol* **15**: 157

966 **Ren G, Meng X, Shuxin Z, Carissa V, Chen X, Bin. Y** (2014) Methylation protects
967 microRNAs from an AGO1-associated activity that uridylates 5' RNA fragments
968 generated by AGO1 cleavage. *Proc Natl Acad Sci* **111**: 6365–6370

969 **Ren Y, Li M, Wang W, Schenke D, Cai D, Miao Y** (2022) MicroRNA840
970 (MIR840) accelerates leaf senescence by targeting the overlapping 3'UTRs of PPR
971 and WHIRLY3 in *Arabidopsis thaliana*. *Plant J* **109**: 126–143

972 **Somvanshi PR, Patel AK, Bhartiya S, Venkatesh K V.** (2015) Implementation of
973 integral feedback control in biological systems. *Wiley Interdiscip Rev Syst Biol Med*
974 **7**: 301–316

975 **Song L, Huang SC, Wise A, Castanon R, Nery JR, Chen H, Watanabe M, Thomas J, Bar-**
976 **Joseph Z, Ecker JR** (2016) A transcription factor hierarchy defines an
977 environmental stress response network. *Science*. doi: 10.1126/science.aag1550

978 **Sorenson RS, Deshotal MJ, Johnson K, Adler FR, Sieburth LE** (2018) *Arabidopsis*
979 mRNA decay landscape arises from specialized RNA decay substrates, decapping-
980 mediated feedback, and redundancy. *Proc Natl Acad Sci U S A* **115**: E1485–E1494

981 **Souret FF, Kastenmayer JP, Green PJ** (2004) AtXRN4 Degrades mRNA in *Arabidopsis*
982 and Its Substrates Include Selected miRNA Targets. *Mol Cell* **15**: 173–183

983 **Teale WD, Paponov IA, Palme K** (2006) Auxin in action: signalling, transport and the
984 control of plant growth and development. *Nat Rev Mol Cell Biol* **7**: 847–859

985 **Tischer S V, Wunschel C, Papacek M, Kleigrewe K, Hofmann T, Christmann A, Grill**
986 **E** (2017) Combinatorial interaction network of abscisic acid receptors and
987 coreceptors from *Arabidopsis thaliana*. *Proc Natl Acad Sci U S A* **114**: 10280–10285

988 **Umezawa T, Sugiyama N, Mizoguchi M, Hayashi S, Myouga F, Yamaguchi-Shinozaki**
989 **K, Ishihama Y, Hirayama T, Shinozaki K** (2009) Type 2C protein phosphatases
990 directly regulate abscisic acid-activated protein kinases in *Arabidopsis*. *Proc Natl*
991 *Acad Sci U S A* **106**: 17588–93

992 **Urano K, Maruyama K, Jikumaru Y, Kamiya Y, Yamaguchi-Shinozaki K, Shinozaki K**
993 **(2017) Analysis of plant hormone profiles in response to moderate dehydration**
994 **stress. Plant J** **90**: 17–36

995 **Varkonyi-Gasic E, Wu R, Wood M, Walton EF, Hellens RP** (2007) Protocol: a highly
996 sensitive RT-PCR method for detection and quantification of microRNAs. *Plant*
997 *Methods* **3**: 12

998 **Vazquez F, Gascioli V, Crété P, Vaucheret H** (2004) The Nuclear dsRNA Binding
999 Protein HYL1 Is Required for MicroRNA Accumulation and Plant Development, but
1000 Not Posttranscriptional Transgene Silencing. *Curr Biol*. doi:
1001 10.1016/j.cub.2004.01.035

1002 **Wang J-W, Czech B, Weigel D** (2009) miR156-Regulated SPL Transcription Factors
1003 Define an Endogenous Flowering Pathway in *Arabidopsis thaliana*. *Cell* **138**: 738–
1004 749

1005 **Wang P, Xue L, Batelli G, Lee S, Hou Y-J, Van Oosten MJ, Zhang H, Tao WA, Zhu J-K**
1006 **(2013) Quantitative phosphoproteomics identifies SnRK2 protein kinase substrates**
1007 **and reveals the effectors of abscisic acid action. Proc Natl Acad Sci U S A** **110**:
1008 11205–10

1009 **Wang Z, Ji H, Yuan B, Wang S, Su C, Yao B, Zhao H, Li X** (2015) ABA signalling is fine-
1010 tuned by antagonistic HAB1 variants. *Nat Commun* **6**: 8138

1011 **Waters MT, Gutjahr C, Bennett T, Nelson DC** (2017) Strigolactone Signaling and
1012 Evolution. *Annu Rev Plant Biol* **68**: 291–322

1013 **Wawer I, Golisz A, Sulkowska A, Kawa D, Kulik A, Kufel J** (2018) mRNA decapping

1014 and 5'-3' decay contribute to the regulation of ABA signaling in *Arabidopsis*
1015 *thaliana*. *Front Plant Sci* **9**: 312

1016 **Xu J, Chua N-H** (2009) *Arabidopsis* decapping 5 is required for mRNA decapping, P-
1017 body formation, and translational repression during postembryonic development.
1018 *Plant Cell* **21**: 3270–9

1019 **Yoshida T, Christmann A, Yamaguchi-Shinozaki K, Grill E, Fernie AR** (2019)
1020 Revisiting the Basal Role of ABA - Roles Outside of Stress. *Trends Plant Sci*. doi:
1021 10.1016/j.tplants.2019.04.008

1022 **Yoshida T, Fujita Y, Maruyama K, Mogami J, Todaka D, Shinozaki K, Yamaguchi-
1023 Shinozaki K** (2015) Four *Arabidopsis* AREB/ABF transcription factors function
1024 predominantly in gene expression downstream of SnRK2 kinases in abscisic acid
1025 signalling in response to osmotic stress. *Plant Cell Environ* **38**: 35–49

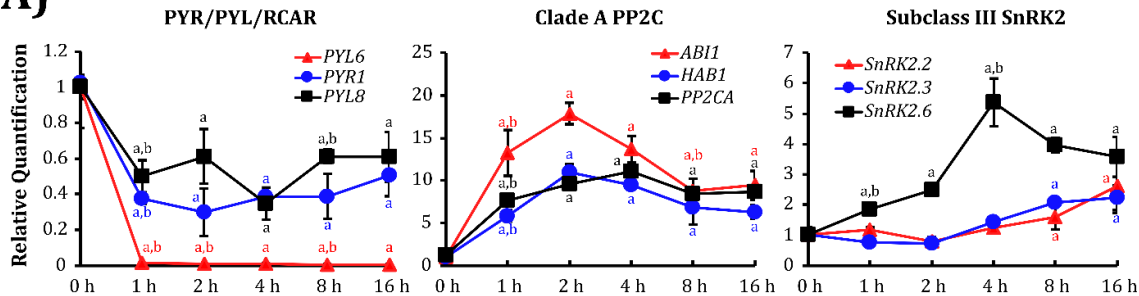
1026 **Zhao Y, Zhang Z, Gao J, Wang P, Hu T, Wang Z, Hou YJ, Wan Y, Liu W, Xie S, et al**
1027 (2018) *Arabidopsis* Duodecuple Mutant of PYL ABA Receptors Reveals PYL
1028 Repression of ABA-Independent SnRK2 Activity. *Cell Rep* **23**: 3340-3351.e5

1029 **Zheng Z, Reichel M, Deveson I, Wong G, Li J, Millar AA** (2017) Target RNA Secondary
1030 Structure Is a Major Determinant of miR159 Efficacy. *Plant Physiol* **174**: 1764–1778

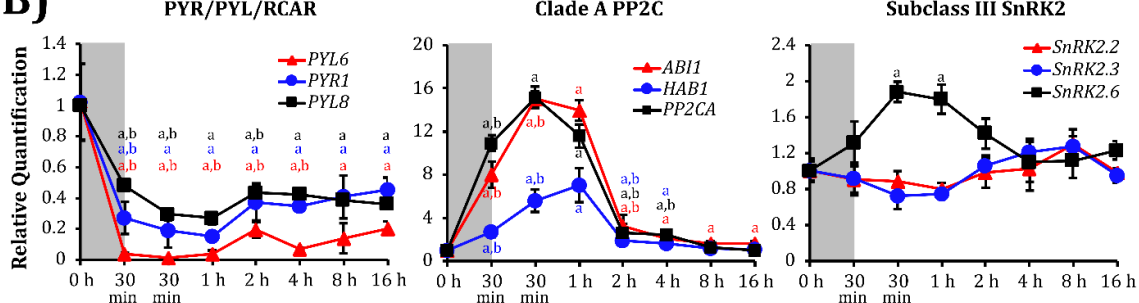
1031 **Zhu J-Y, Sae-Seaw J, Wang Z-Y** (2013) Brassinosteroid signalling. *Development* **140**:
1032 1615–20

1033

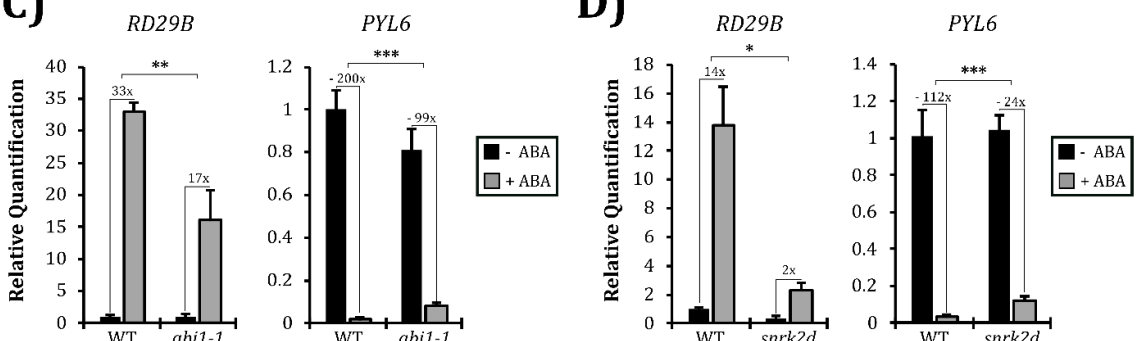
A)



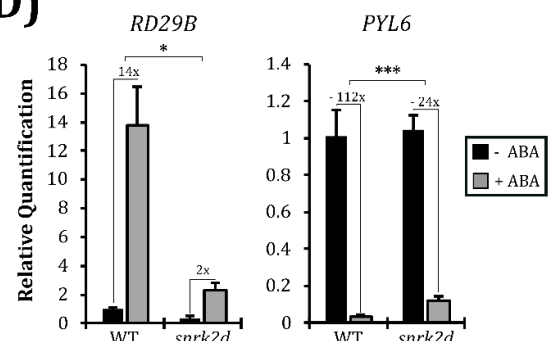
B)



C)



D)



E)

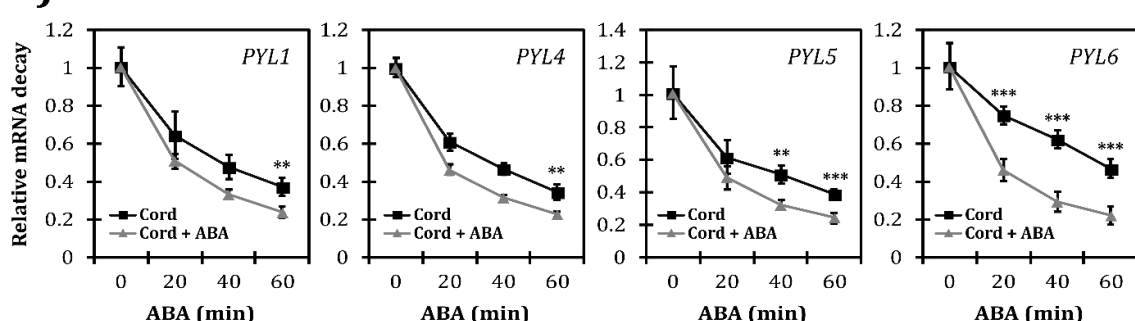


Figure 1: Regulation of the expression of ABA core signaling pathway genes by ABA.

(A) mRNA profile of members of the ABA core signaling pathway in response to long-term ABA treatment. One member of each subgroup of PYR/PYL/RCAR and three members of clade A PP2Cs (Supplemental Fig. S1A) are represented, along with subclass III SnRK2 members. An expanded analysis with PYR/PYL/RCAR and PP2C genes is given in Supplemental Fig. S2. Seedlings were treated with 1 μ M ABA for up to 16 hours.

(B) mRNA profile of members of the ABA core signaling pathway in response to transient ABA-treatment. Seedlings were treated with 1 μ M ABA for 30 min, then ABA was removed from the medium. Sampling was performed before the treatment (0 h), at the end of the 30 min (in the gray

bioRxiv preprint doi: <https://doi.org/10.1101/2023.01.17.524441>; this version posted January 21, 2023. The copyright holder for this preprint (which was not certified by peer review) is the author/funder, who has granted bioRxiv a license to display the preprint in perpetuity. It is made available under aCC-BY-NC-ND 4.0 International license.

box) of ABA-treatment, and at different time points after hormone removal. An expanded analysis with *PYR/PYL/RCAR* and *PP2C* genes is given in Supplemental Fig. S3.

In panels A and B “a” means significant difference between each time point vs the untreated control and “b” each time point vs. the previous one. Responses were significantly different for fold changes in mRNA levels $\geq |1.5|$ and $p < 0.05$, according to Student's t-test. The color of the letter refers to the gene evaluated.

(C) The negative feedback regulation of the ABA core signaling pathway requires ABA-signalization. Wild type (WT) and *abi1-1* seedlings were treated with 1 μ M ABA for 1 hour before sampling. Expression of the ABA-induced *Rd29B* gene was used as positive control of ABA-promoted responses. *PYL6* response is shown and a complete analysis of the expression of six other representative ABA receptors is provided in Supplemental Fig. S4. The expression levels are given in comparison to the untreated WT.

(D) Kinases SnRK2 are involved in the negative feedback of *PYR/PYL/RCAR* genes in response to ABA. WT and the double kinase mutant *snrk2.2/snr2.3* (*snrk2d*) seedlings were treated with 1 μ M ABA for 1 hour before sampling. Expression of the ABA-induced *Rd29B* gene was used as positive control of ABA-promoted responses. *PYL6* response is shown and a complete analysis of the expression of the six other representative ABA receptors is provided in Supplemental Fig. S6. The expression levels are given in comparison to the untreated WT.

(E) ABA regulates *PYL1*, *PYL4*, *PYL5* and *PYL6* mRNA stability. To evaluate ABA-mediated control of mRNA stability, seedlings were pre-treated for 1 h with 100 μ M cordycepin (Cord) to inhibit transcription, followed by the addition of ABA 1 μ M (Cord + ABA). After cordycepin pre-treatment sampling was performed at 20, 40 and 60 minutes with and without ABA. Relative expression values in Cord + ABA condition that are lower than the respective Cord treatment alone indicate that the stability of the transcript was decreased in response to ABA. A complete analysis of the mRNA stability of representative *PYR/PYL/RCAR* genes is given in Supplemental Table S3.

For all experiments, values are the mean of five biological replicates \pm standard deviation. Responses were significantly different for fold changes in mRNA levels $\geq |1.5|$ and $p < 0.05$, according to Student's t-test (* < 0.05 ; ** < 0.005 ; *** < 0.0005).

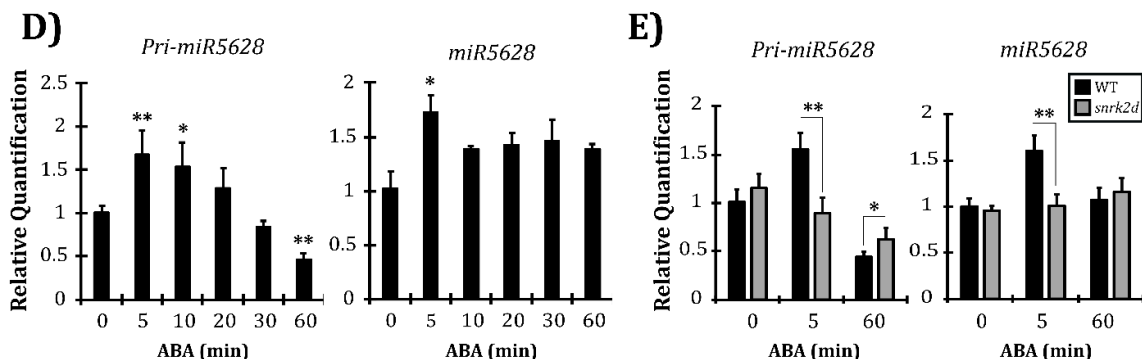
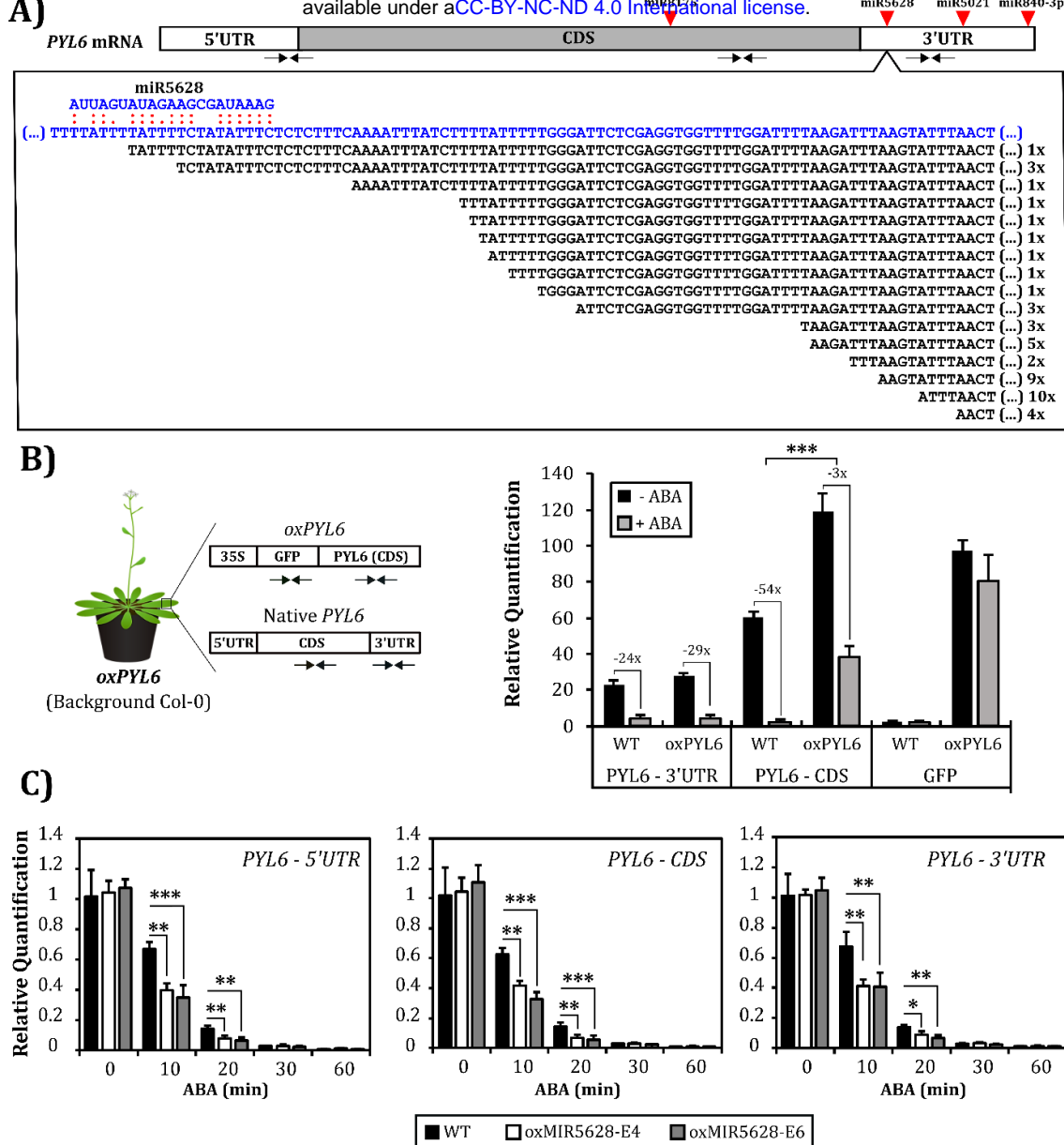


Figure 2: MiR5628 promotes cleavage of PYL6 mRNA in response to ABA.

(A) Schematic representation of *PYL6* mRNA with the putative miR8175, miR5628, miR5021 and miR840-3p and the position of their binding sites in *PYL6* mRNA. 5'-RACE analysis of *PYL6* mRNA cleavage by miR5628 in Col-0. Forty-seven cloned sequences (in black) mapped to the miR5628 recognition site (position 784-804 bp of *PYL6* mRNA) or downstream of it in the 3'UTR sequence (blue). The number of occurrences of each sequence is indicated.

(B) The 3'UTR of *PYL6* transcript is required for proper control of its stability in response to ABA.

The relative amounts of the CDS and 3'UTR sequences of *PYL6* mRNA was quantified in wild type (WT) and in a transgenic line expressing the 35S:GFP:PYL6 (Col-0 background), which lacks the *PYL6* 3'UTR region (*oxPYL6*). Amplification of *GFP* sequence allows to quantify specifically the *oxPYL6* fusion. Fourteen days old seedlings grown under continuous light were treated with 1 μ M ABA for 30 min. This analyze is representative of three independent experiments.

(C) miR5628 participates in the degradation of *PYL6* transcript in response to ABA. The amount of *PYL6*-5'UTR, CDS and 3'UTR sequences (primers positions are shown in panel A) was quantified at different time points of a 60 min treatment with 1 μ M ABA in samples of oxMIR5628 (E4 and E6) and WT seedlings. Relative expression values of each genotype were obtained in comparison to the untreated WT. This analyze is representative of two independent experiments.

(D) ABA transiently induces both the *pri-miR5628* and the mature *miR5628*. Col-0 seedlings were treated with 1 μ M ABA and sampling was performed before (0 min) and at 5, 10, 20, 30 and 60 minutes after ABA application. Relative expression values were obtained in comparison to the untreated condition (time point of 0 min). This analyze is representative of four independent experiments.

(E) A functional ABA signaling is required to transient induction of *pri-miR5628* and the mature *miR5628* in response to ABA. WT and the double kinase mutant *snrk2d* (*snrk2.2/snr2.3*) seedlings were treated with 1 μ M ABA and sampling was performed before (0 min), at 5 and 60 minutes after ABA application. The relative expression levels are given in comparison to the untreated WT.

In panels B, C, D and E, values are the means of five biological replicates \pm standard deviation. RT-qPCR was carried out to gene quantification. Responses were significantly different for fold changes in mRNA levels $\geq |1.5|$ and $p < 0.05$, according to Student's t-test (* < 0.05 ; ** < 0.005 ; *** < 0.0005).

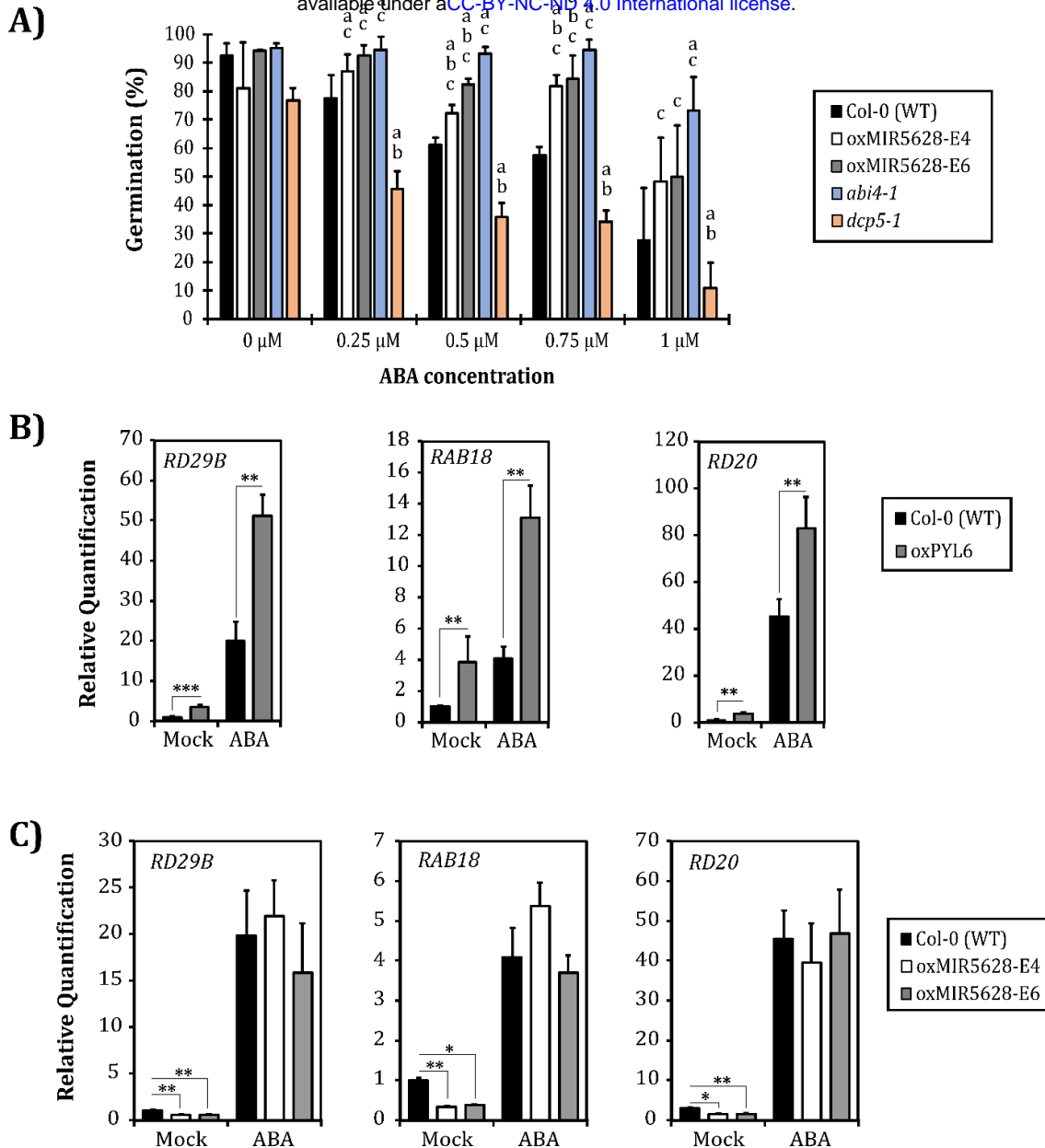


Figure 3: miR5628 impacts ABA signaling.

(A) oxMIR5628 lines are hyposensitive to ABA during germination. The germination rate of WT, oxMIR5628 lines, *abi4-1* and *dcp5-1* genotypes were evaluated in continuous light on solid (0.25% of agar) MS/2 medium along a range of ABA concentrations (0, 0.25, 0.5, 0.75 e 1 μ M of ABA). The data represent the average of three biological replicates (three plates) with at least 30 seeds for each genotype. Seeds germination was monitored during six days after exposure to light. The seed germination rate (%) corresponds to the number of seeds that germinated each day for the total of seeds germinated at the sixth day. The graphic represents the differences observed at the second day. The mutants *abi4-1* and *dcp5-1* were used as control for ABA-hypo and -hypersensitive phenotypes, respectively. Responses were significantly different for changes in the germination rate according to Tukey and Scott-Knott test, which is represented by the letters "a" (statistical difference in relation to WT), "b" (statistical difference in relation to *abi4-1*) and "c" (statistical difference in relation to *dcp5-1*). This analyze is representative of two independent experiments.

(B) ABA signaling readout genes (*RD29B*, *RAB18* and *RD20*) are upregulated in the *oxPYL6* genotype both in the presence and absence of ABA. WT and *oxPYL6* seedlings were treated with 1 μ M ABA for 1 hour before sampling. Relative expression values of each genotype were obtained in comparison to the untreated WT. This analyze is representative of three independent experiments.

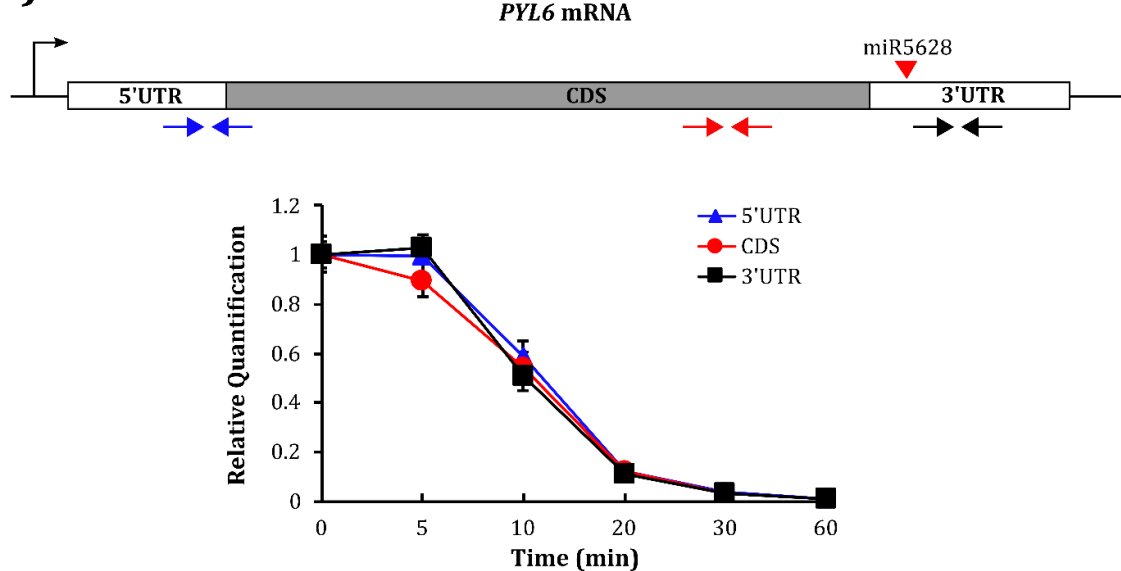
(C) ABA signaling readout genes (*RD29B*, *RAB18* and *RD20*) are downregulated in the oxMIR5628 lines. WT and oxMIR5628 (E4 and E6) seedlings were treated with 1 μ M ABA for 1 hour before

bioRxiv preprint doi: <https://doi.org/10.1101/2023.01.17.524441>; this version posted January 21, 2023. The copyright holder for this preprint (which was not certified by peer review) is the author/funder, who has granted bioRxiv a license to display the preprint in perpetuity. It is made available under a [aCC-BY-NC-ND 4.0 International license](#).

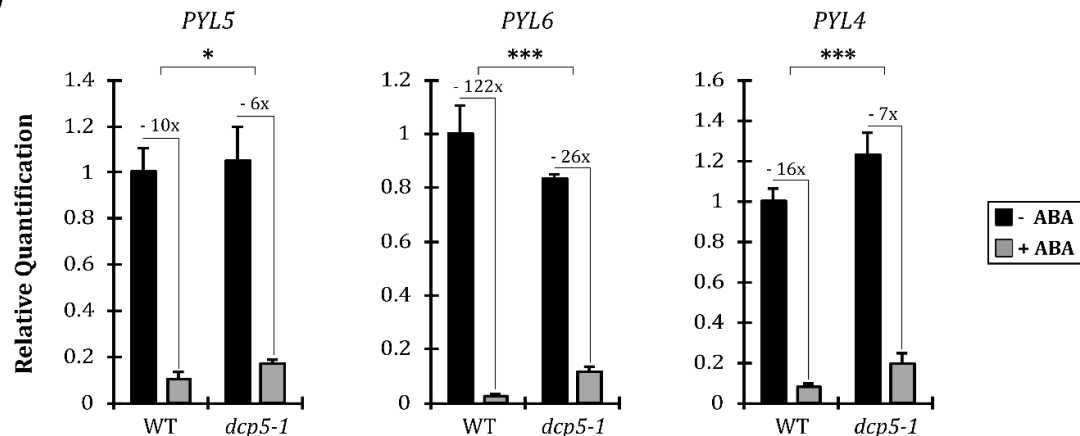
sampling. Relative expression values of each genotype were obtained in comparison to the untreated WT. This analyze is representative of three independent experiments.

In panels B and C, values are the means of five biological replicates \pm standard deviation. RT-qPCR was carried out to gene quantification. Responses were considered to be significantly different for fold changes in mRNA levels $\geq |1.5|$ and $p < 0.05$, according to Student's t-test (* < 0.05 ; ** < 0.005 ; *** < 0.0005).

A)



B)



C)

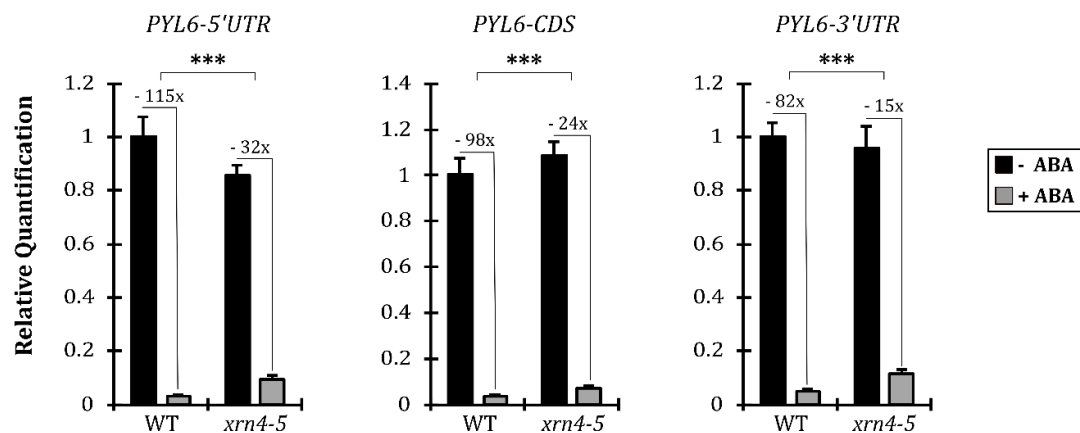


Figure 4: 5'-3' mRNA decay pathway is involved in the control of *PYL6* mRNA accumulation in response to ABA.

(A) Schematic representation of *PYL6* mRNA with the 5'- and 3'-UTRs and coding sequence (CDS) regions, and miR5628 target site. The position of primer pairs that were used to measure the level of mRNA corresponding to different parts of *PYL6* transcript are shown. The different regions of *PYL6* were quantified by RT-qPCR along a time course of ABA treatment. Seedlings were grown for six days

bioRxiv preprint doi: <https://doi.org/10.1101/2023.01.17.524441>; this version posted January 21, 2023. The copyright holder for this preprint (which was not certified by peer review) is the author/funder, who has granted bioRxiv a license to display the preprint in perpetuity. It is made available under a [CC-BY-NC-ND 4.0 International license](#).

and were treated with 1 μ M ABA. Sampling was performed before (0 min) and at 5, 10, 20, 30 and 60 min after ABA application. This analysis is representative of three independent experiments.

(B) *PYL4*, *PYL5* and *PYL6* transcripts profiles were compared between the mutant *dcp5-1*, which is defective in decapping activity, and the wild type (WT) in response to ABA treatment.

(C) Accumulation of 5'UTR, CDS and 3'UTR regions of *PYL6* mRNA compared between *xrn4-5* mutant and WT in response to ABA. This analysis represents three independent experiments.

In panels B and C, seedlings were treated with 1 μ M ABA for 1 hour before sampling. Values are the means of five biological replicates \pm standard deviation. The relative levels of transcripts were obtained in comparison to the untreated WT. Responses were significantly different for fold changes in mRNA levels $\geq |1.5|$ and $p < 0.05$, according to Student's t-test (* < 0.05 ; ** < 0.005 ; *** < 0.0005).

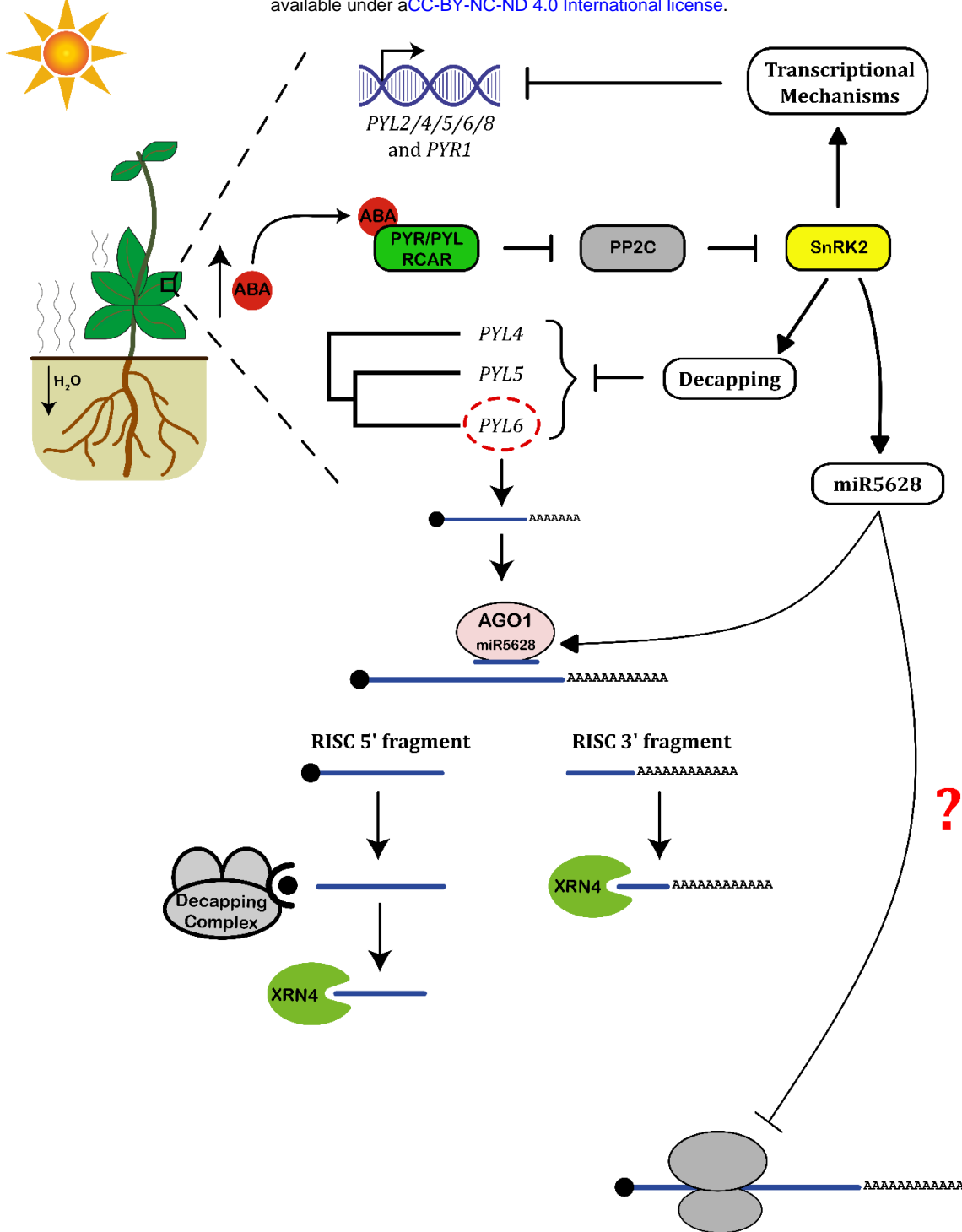


Figure 5: Model of the control of ABA signalization through repression of *PYR/PYL/RCAR* genes. Abiotic stress conditions such as drought, increase the endogenous level of ABA, which is perceived by PYR/PYL/RCAR receptors. The ABA-receptor complex sequesters Clade A PP2C phosphatases, releasing SnRK2 kinases from their negative regulation. These SnRK2s phosphorylate several proteins in order to activate the gene expression program of ABA responses. Part of these ABA responses are involved in the transcriptional repression of *PYL1/2/4/5/6* and *PYR1* genes. In addition, ABA accelerates the decay of *PYL1/4/5/6* transcripts. The ABA core signaling pathway induces miR5628 expression, which in turn is processed and loaded onto AGO1. AGO1-miR5628 complex promotes the cleavage of *PYL6* mRNA at the 3'UTR region, and XRN4 promotes the degradation of the RISC 3'-cleaved fragment of *PYL6*. Additionally, the dynamic of *PYL6* mRNA decay may involve the participation of 5' to 3' mRNA decay pathway, where RISC 5'-cleaved fragment of

PYL6 transcripts would undergo decapping followed by ARN1-mediated degradation. Decapping may also contribute to destabilize *PYL4* and *PYL5* transcripts, which are phylogenetically close to *PYL6*. The repression of *PYR/PYL/RCAR* genes expression is a mean to limit de novo synthesis of receptors, controlling the extension of ABA responses and participating in the resetting of the ABA signaling. In addition, it might be possible that miR5628 would regulate *PYL6* mRNA translation.

Parsed Citations

Axtell MJ (2013) Classification and comparison of small RNAs from plants. *Annu Rev Plant Biol* 64: 137–159

Google Scholar: [Author Only](#) [Title Only](#) [Author and Title](#)

Barrera-Rojas CH, Otoni WC, Nogueira FTS (2021) Shaping the root system: the interplay between miRNA regulatory hubs and phytohormones. *J Exp Bot* 72: 6822–6835

Google Scholar: [Author Only](#) [Title Only](#) [Author and Title](#)

Belda-Palazon B, Rodriguez L, Fernandez MA, Castillo M-C, Anderson EA, Gao C, González-Guzmán M, Peirats-Llobet M, Zhao Q, De Winne N, et al (2016) FYVE1/FREE1 Interacts with the PYL4 ABA Receptor and Mediates its Delivery to the Vacuolar Degradation Pathway. *Plant Cell* 28: tpc.00178.2016

Google Scholar: [Author Only](#) [Title Only](#) [Author and Title](#)

Chantarachot T, Bailey-Serres J (2018) Polysomes, Stress Granules, and Processing Bodies: A Dynamic Triumvirate Controlling Cytoplasmic mRNA Fate and Function. *Plant Physiol* 176: 254–269

Google Scholar: [Author Only](#) [Title Only](#) [Author and Title](#)

Chen H-H, Qu L, Xu Z-H, Zhu J-K, Xue H-W (2018) EL1-like Casein Kinases Suppress ABA Signaling and Responses by Phosphorylating and Destabilizing the ABA Receptors PYR/PYLs in *Arabidopsis*. *Mol Plant* 11: 706–719

Google Scholar: [Author Only](#) [Title Only](#) [Author and Title](#)

Chu LH, Jeng ST (2002) Multiple transduction pathways regulate the 35S promoter with an ABA responsive element. *Plant Sci* 163: 23–32

Google Scholar: [Author Only](#) [Title Only](#) [Author and Title](#)

Czechowski T, Stitt M, Altmann T, Udvardi MK, Scheible W-R (2005) Genome-wide identification and testing of superior reference genes for transcript normalization in *Arabidopsis*. *Plant Physiol* 139: 5–17

Google Scholar: [Author Only](#) [Title Only](#) [Author and Title](#)

Dai X, Zhuang Z, Zhao PX (2018) psRNATarget: a plant small RNA target analysis server (2017 release). *Nucleic Acids Res* 46: W49–W54

Google Scholar: [Author Only](#) [Title Only](#) [Author and Title](#)

Davière J-M, Achard P (2013) Gibberellin signaling in plants. *Development* 140: 1147–1151

Google Scholar: [Author Only](#) [Title Only](#) [Author and Title](#)

Duarte GT, Matiolli CC, Pant BD, Schlereth A, Scheible W-R, Stitt M, Vicentini R, Vincentz M (2013) Involvement of microRNA-related regulatory pathways in the glucose-mediated control of *Arabidopsis* early seedling development. *J Exp Bot* 64: 4301–4312

Google Scholar: [Author Only](#) [Title Only](#) [Author and Title](#)

Fahlgren N, Howell MD, Kasschau KD, Chapman EJ, Sullivan CM, Cumbie JS, Givan SA, Law TF, Grant SR, Dangl JL, et al (2007) High-Throughput Sequencing of *Arabidopsis* microRNAs: Evidence for Frequent Birth and Death of MIRNA Genes. *PLoS One* 2: e219

Google Scholar: [Author Only](#) [Title Only](#) [Author and Title](#)

Fahlgren N, Jogdeo S, Kasschau KD, Sullivan CM, Chapman EJ, Laubinger S, Smith LM, Dasenko M, Givan SA, Weigel D, et al (2012) MicroRNA Gene Evolution in *Arabidopsis lyrata* and *Arabidopsis thaliana*. *Plant Cell* 22: 1074–1089

Google Scholar: [Author Only](#) [Title Only](#) [Author and Title](#)

Feng L, Zhang F, Zhang H, Zhao Y, Meyers BC, Zhai J (2020) An Online Database for Exploring Over 2,000 *Arabidopsis* Small RNA Libraries. *Plant Physiol* 182: 685–691

Google Scholar: [Author Only](#) [Title Only](#) [Author and Title](#)

Finkelstein RR (1994) Mutations at two new *Arabidopsis* ABA response loci are similar to the *abi3* mutations. *Plant J* 5: 765–771

Google Scholar: [Author Only](#) [Title Only](#) [Author and Title](#)

Fujii H, Verslues PE, Zhu JK (2007) Identification of Two Protein Kinases Required for Abscisic Acid Regulation of Seed Germination, Root Growth, and Gene Expression in *Arabidopsis*. *Plant Cell* 19: 485–494

Google Scholar: [Author Only](#) [Title Only](#) [Author and Title](#)

Fujita Y, Nakashima K, Yoshida T, Katagiri T, Kidokoro S, Kanamori N, Umezawa T, Fujita M, Maruyama K, Ishiyama K, et al (2009) Three SnRK2 Protein Kinases are the Main Positive Regulators of Abscisic Acid Signaling in Response to Water Stress in *Arabidopsis*. *Plant Cell Physiol* 50: 2123–2132

Google Scholar: [Author Only](#) [Title Only](#) [Author and Title](#)

Gandikota M, Birkenbihl RP, Höhmann S, Cardon GH, Saedler H, Huijser P (2007) The miRNA156/157 recognition element in the 3' UTR of the *Arabidopsis* SBP box gene SPL3 prevents early flowering by translational inhibition in seedlings. *Plant J* 49: 683–693

Google Scholar: [Author Only](#) [Title Only](#) [Author and Title](#)

Gou X, Zhong C, Zhang P, Mi L, Li Y, Lu W, Zheng J, Xu J, Meng Y, Shan W (2022) miR398b and AtC2GnT form a negative feedback loop to regulate *Arabidopsis thaliana* resistance against *Phytophthora parasitica*. *Plant J* 111: 360–373

Google Scholar: [Author Only](#) [Title Only](#) [Author and Title](#)

Gruber AR, Lorenz R, Bernhart SH, Neubock R, Hofacker IL (2008) The Vienna RNA Websuite. *Nucleic Acids Res* 36: W70–W74

Google Scholar: [Author Only](#) [Title Only](#) [Author and Title](#)

Hajieghrari B, Farrokhi N (2021) Investigation on the Conserved MicroRNA Genes in Higher Plants. *Plant Mol Biol Report* 39: 10–23

Google Scholar: [Author Only](#) [Title Only](#) [Author and Title](#)

Irigoyen ML, Iniesto E, Rodriguez L, Puga MI, Yanagawa Y, Pick E, Strickland E, Paz-Ares J, Wei N, De Jaeger G, et al (2014) Targeted degradation of abscisic acid receptors is mediated by the ubiquitin ligase substrate adaptor DDA1 in *Arabidopsis*. *Plant Cell* 26: 712–28

Google Scholar: [Author Only](#) [Title Only](#) [Author and Title](#)

Iwakawa H oki, Tomari Y (2013) Molecular Insights into microRNA-Mediated Translational Repression in Plants. *Mol Cell* 52: 591–601

Google Scholar: [Author Only](#) [Title Only](#) [Author and Title](#)

Kavi Kishor PB, Tiozon RN, Fernie AR, Sreenivasulu N (2022) Abscisic acid and its role in the modulation of plant growth, development, and yield stability. *Trends Plant Sci* 27: 1283–1295

Google Scholar: [Author Only](#) [Title Only](#) [Author and Title](#)

Kieber JJ, Schaller GE (2018) Cytokinin signaling in plant development. *Development* 145: dev149344

Google Scholar: [Author Only](#) [Title Only](#) [Author and Title](#)

Klepikova AV, Kasianov AS, Gerasimov ES, Logacheva MD, Penin AA (2016) A high resolution map of the *Arabidopsis thaliana* developmental transcriptome based on RNA-seq profiling. *Plant J* 88: 1058–1070

Google Scholar: [Author Only](#) [Title Only](#) [Author and Title](#)

Kumar S, Stecher G, Tamura K (2016) MEGA7: Molecular Evolutionary Genetics Analysis Version 7.0 for Bigger Datasets. *Mol Biol Evol* 33: 1870–1874

Google Scholar: [Author Only](#) [Title Only](#) [Author and Title](#)

Lee HJ, Park YJ, Kwak KJ, Kim D, Park JH, Lim JY, Shin C, Yang KY, Kang H (2015) MicroRNA844-guided downregulation of cytidinephosphate diacylglycerol Synthase3 (CDS3) mRNA affects the response of *arabidopsis thaliana* to bacteria and fungi. *Mol Plant-Microbe Interact* 28: 892–900

Google Scholar: [Author Only](#) [Title Only](#) [Author and Title](#)

Li D, Zhang L, Li X, Kong X, Wang X, Li Y, Liu Z, Wang J, Li X, Yang Y (2018) AtRAE1 is involved in degradation of ABA receptor RCAR1 and negatively regulates ABA signalling in *Arabidopsis*. *Plant Cell Environ* 41: 231–244

Google Scholar: [Author Only](#) [Title Only](#) [Author and Title](#)

Liu Q, Wang F, Axtell MJ (2014) Analysis of complementarity requirements for plant microRNA targeting using a *Nicotiana benthamiana* quantitative transient assay. *Plant Cell* 26: 741–53

Google Scholar: [Author Only](#) [Title Only](#) [Author and Title](#)

Ma Y, Szostkiewicz I, Korte A, Moes D, Yang Y, Christmann A, Grill E (2009) Regulators of PP2C Phosphatase Activity Function as Abscisic Acid Sensors. *Science* (80-) 324: 1064–1069

Google Scholar: [Author Only](#) [Title Only](#) [Author and Title](#)

Matiolli CC, Tomaz JP, Duarte GT, Prado FM, Del Bem LEV, Silveira AB, Gauer L, Corrêa LGG, Drumond RD, Viana AJC, et al (2011) The *Arabidopsis* bZIP gene AtbZIP63 is a sensitive integrator of transient abscisic acid and glucose signals. *Plant Physiol* 157: 692–705

Google Scholar: [Author Only](#) [Title Only](#) [Author and Title](#)

Mi S, Cai T, Hu Y, Chen Y, Hodges E, Ni F, Wu L, Li S, Zhou H, Long C, et al (2008) Sorting of small RNAs into *Arabidopsis* argonaute complexes is directed by the 5' terminal nucleotide. *Cell* 133: 116–127

Google Scholar: [Author Only](#) [Title Only](#) [Author and Title](#)

Morel J-BJ-B, Godon C, Mourrain P, Béclin C, Boutet S, Feuerbach F, Proux F, Vaucheret H (2002) Fertile hypomorphic ARGONAUTE (ago1) mutants impaired in post-transcriptional gene silencing and virus resistance. *Plant Cell* 14: 629–39

Google Scholar: [Author Only](#) [Title Only](#) [Author and Title](#)

Mugridge JS, Coller J, Gross JD (2018) Structural and molecular mechanisms for the control of eukaryotic 5'–3' mRNA decay. *Nat Struct Mol Biol* 25: 1077–1085

Google Scholar: [Author Only](#) [Title Only](#) [Author and Title](#)

Park S, Fung P, Nishimura N, Jensen DR, Fujii H, Zhao Y, Lumba S, Santiago J, Rodrigues A, Chow TF, et al (2009) Abscisic Acid

Inhibits Type 2C Protein Phosphatases via the PYR/PYL Family of START Proteins. *Science* (80-) 324: 1068–1069

Google Scholar: [Author Only](#) [Title Only](#) [Author and Title](#)

Rai MI, Wang X, Thibault DM, Kim HJ, Bombyk MM, Binder BM, Shakeel SN, Schaller GE (2015) The ARGOS gene family functions in a negative feedback loop to desensitize plants to ethylene. *BMC Plant Biol* 15: 157

Google Scholar: [Author Only](#) [Title Only](#) [Author and Title](#)

Ren G, Meng X, Shuxin Z, Carissa V, Chen X, Bin. Y (2014) Methylation protects microRNAs from an AGO1-associated activity that uridylates 5' RNAfragments generated by AGO1 cleavage. *Proc Natl Acad Sci* 111: 6365–6370

Google Scholar: [Author Only](#) [Title Only](#) [Author and Title](#)

Ren Y, Li M, Wang W, Lan W, Schenke D, Cai D, Miao Y (2022) MicroRNA840 (MIR840) accelerates leaf senescence by targeting the overlapping 3'UTRs of PPR and WHIRLY3 in *Arabidopsis thaliana*. *Plant J* 109: 126–143

Google Scholar: [Author Only](#) [Title Only](#) [Author and Title](#)

Somvanshi PR, Patel AK, Bhartiya S, Venkatesh K V. (2015) Implementation of integral feedback control in biological systems. *Wiley Interdiscip Rev Syst Biol Med* 7: 301–316

Google Scholar: [Author Only](#) [Title Only](#) [Author and Title](#)

Song L, Huang SC, Wise A, Castanon R, Nery JR, Chen H, Watanabe M, Thomas J, Bar-Joseph Z, Ecker JR (2016) A transcription factor hierarchy defines an environmental stress response network. *Science*. doi: 10.1126/science.aag1550

Google Scholar: [Author Only](#) [Title Only](#) [Author and Title](#)

Sorenson RS, Desholt MJ, Johnson K, Adler FR, Sieburth LE (2018) *Arabidopsis* mRNA decay landscape arises from specialized RNA decay substrates, decapping-mediated feedback, and redundancy. *Proc Natl Acad Sci U S A* 115: E1485–E1494

Google Scholar: [Author Only](#) [Title Only](#) [Author and Title](#)

Souret FF, Kastenmayer JP, Green PJ (2004) AtXRN4 Degrades mRNA in *Arabidopsis* and Its Substrates Include Selected miRNA Targets. *Mol Cell* 15: 173–183

Google Scholar: [Author Only](#) [Title Only](#) [Author and Title](#)

Teale WD, Paponov IA, Palme K (2006) Auxin in action: signalling, transport and the control of plant growth and development. *Nat Rev Mol Cell Biol* 7: 847–859

Google Scholar: [Author Only](#) [Title Only](#) [Author and Title](#)

Tischer S V, Wunschel C, Papacek M, Kleigrewe K, Hofmann T, Christmann A, Grill E (2017) Combinatorial interaction network of abscisic acid receptors and coreceptors from *Arabidopsis thaliana*. *Proc Natl Acad Sci U S A* 114: 10280–10285

Google Scholar: [Author Only](#) [Title Only](#) [Author and Title](#)

Umezawa T, Sugiyama N, Mizoguchi M, Hayashi S, Myouga F, Yamaguchi-Shinozaki K, Ishihama Y, Hirayama T, Shinozaki K (2009) Type 2C protein phosphatases directly regulate abscisic acid-activated protein kinases in *Arabidopsis*. *Proc Natl Acad Sci U S A* 106: 17588–93

Google Scholar: [Author Only](#) [Title Only](#) [Author and Title](#)

Urano K, Maruyama K, Jikumaru Y, Kamiya Y, Yamaguchi-Shinozaki K, Shinozaki K (2017) Analysis of plant hormone profiles in response to moderate dehydration stress. *Plant J* 90: 17–36

Google Scholar: [Author Only](#) [Title Only](#) [Author and Title](#)

Varkonyi-Gasic E, Wu R, Wood M, Walton EF, Hellens RP (2007) Protocol: a highly sensitive RT-PCR method for detection and quantification of microRNAs. *Plant Methods* 3: 12

Google Scholar: [Author Only](#) [Title Only](#) [Author and Title](#)

Vazquez F, Gascioli V, Crété P, Vaucheret H (2004) The Nuclear dsRNA Binding Protein HYL1 Is Required for MicroRNA Accumulation and Plant Development, but Not Posttranscriptional Transgene Silencing. *Curr Biol*. doi: 10.1016/j.cub.2004.01.035

Google Scholar: [Author Only](#) [Title Only](#) [Author and Title](#)

Wang J-W, Czech B, Weigel D (2009) miR156-Regulated SPL Transcription Factors Define an Endogenous Flowering Pathway in *Arabidopsis thaliana*. *Cell* 138: 738–749

Google Scholar: [Author Only](#) [Title Only](#) [Author and Title](#)

Wang P, Xue L, Batelli G, Lee S, Hou Y-J, Van Oosten MJ, Zhang H, Tao WA, Zhu J-K (2013) Quantitative phosphoproteomics identifies SnRK2 protein kinase substrates and reveals the effectors of abscisic acid action. *Proc Natl Acad Sci U S A* 110: 11205–10

Google Scholar: [Author Only](#) [Title Only](#) [Author and Title](#)

Wang Z, Ji H, Yuan B, Wang S, Su C, Yao B, Zhao H, Li X (2015) ABA signalling is fine-tuned by antagonistic HAB1 variants. *Nat Commun* 6: 8138

Google Scholar: [Author Only](#) [Title Only](#) [Author and Title](#)

Waters MT, Gutjahr C, Bennett T, Nelson DC (2017) Strigolactone Signaling and Evolution. *Annu Rev Plant Biol* 68: 291–322

Google Scholar: [Author Only](#) [Title Only](#) [Author and Title](#)

Wawer I, Golisz A, Sulkowska A, Kawa D, Kulik A, Kufel J (2018) mRNA decapping and 5'-3' decay contribute to the regulation of ABA signaling in *Arabidopsis thaliana*. *Front Plant Sci* 9: 312

Google Scholar: [Author Only](#) [Title Only](#) [Author and Title](#)

Xu J, Chua N-H (2009) Arabidopsis decapping 5 is required for mRNA decapping, P-body formation, and translational repression during postembryonic development. *Plant Cell* 21: 3270–9

Google Scholar: [Author Only](#) [Title Only](#) [Author and Title](#)

Yoshida T, Christmann A, Yamaguchi-Shinozaki K, Grill E, Fernie AR (2019) Revisiting the Basal Role of ABA - Roles Outside of Stress. *Trends Plant Sci*. doi: 10.1016/j.tplants.2019.04.008

Google Scholar: [Author Only](#) [Title Only](#) [Author and Title](#)

Yoshida T, Fujita Y, Maruyama K, Mogami J, Todaka D, Shinozaki K, Yamaguchi-Shinozaki K (2015) Four *Arabidopsis* AREB/ABF transcription factors function predominantly in gene expression downstream of SnRK2 kinases in abscisic acid signalling in response to osmotic stress. *Plant Cell Environ* 38: 35–49

Google Scholar: [Author Only](#) [Title Only](#) [Author and Title](#)

Zhao Y, Zhang Z, Gao J, Wang P, Hu T, Wang Z, Hou YJ, Wan Y, Liu W, Xie S, et al (2018) Arabidopsis Duodecuple Mutant of PYL ABA Receptors Reveals PYL Repression of ABA-Independent SnRK2 Activity. *Cell Rep* 23: 3340–3351.e5

Google Scholar: [Author Only](#) [Title Only](#) [Author and Title](#)

Zheng Z, Reichel M, Deveson I, Wong G, Li J, Millar AA (2017) Target RNA Secondary Structure Is a Major Determinant of miR159 Efficacy. *Plant Physiol* 174: 1764–1778

Google Scholar: [Author Only](#) [Title Only](#) [Author and Title](#)

Zhu J-Y, Sae-Seaw J, Wang Z-Y (2013) Brassinosteroid signalling. *Development* 140: 1615–20

Google Scholar: [Author Only](#) [Title Only](#) [Author and Title](#)